Ore Geology Reviews 65 (2015) 1095–1109

Contents lists available at ScienceDirect

Ore Geology Reviews

journal homepage: www.elsevier.com/locate/oregeorev

Determination of germanium isotopic compositions of sulfides by hydride generation MC-ICP-MS and its application to the Pb–Zn deposits in SW China

Yu-Miao Meng [a,b], Hua-Wen Qi [a,*], Rui-Zhong Hu [a]

[a] State Key Laboratory of Ore Deposit Geochemistry, Institute of Geochemistry, Chinese Academy of Sciences, Guiyang 550002, China
[b] University of Chinese Academy of Sciences, Beijing 100049, China

ARTICLE INFO

Article history:
Received 14 February 2014
Received in revised form 1 April 2014
Accepted 14 April 2014
Available online 24 April 2014

Keywords:
Sample preparation
Germanium isotopes
MC-ICP-MS
Sulfides
Pb–Zn deposits

ABSTRACT

Determining Ge isotopic compositions of sulfides is important to understand the ore-forming processes. Single step anion-exchange chromatography was previously used to recover Ge from silicates and lignites. We apply this procedure to recover Ge from sulfides before determining Ge isotopic compositions by hydride generation (HG)-MC-ICP-MS. Germanium is quantitatively recovered by the proposed sample preparation method. There are no obvious isotope biases for Ge-bearing solutions containing significant amounts of Cu, Sn, and W. However, δ^{74}Ge values show obvious shifts if the solutions contain high Zn, Pb, and Sb, which is possibly attributed to suppression of germane formation that fractionates Ge isotopes. The long-term reproducibility for Ge standard solution is about ±0.18‰ for δ^{74}Ge. Spex and Merck standard solutions yield mean δ^{74}Ge values of −0.70 ± 0.19‰ and −0.36 ± 0.08‰, respectively. The calculated δ^{74}Ge value (−5.13‰) of sphalerite standard based on doping experiments is indistinguishable from those of sphalerite without doping (−5.05‰ and −5.01‰). Sulfides from the Jinding, Shanshulin, and Tianqiao Pb–Zn deposits in SW China have δ^{74}Ge values of −4.94‰ to +2.07‰. The paragenetic sequence of sulfides from the Shanshulin and Tianqiao Pb–Zn deposits is pyrite, sphalerite and galena from early to late. Sulfides from the same ore show a trend of $\delta^{74}Ge_{pyrite} < \delta^{74}Ge_{sphalerite} < \delta^{74}Ge_{galena}$, which may be controlled by the kinetic or Rayleigh fractionation.

1. Introduction

Germanium is a trace element with an average content of ~1.6 ppm in the earth's crust (Bernstein, 1985; Rosman and Taylor, 1998). It exhibits lithophile, siderophile, chalcophile, and organophile affinities in different geochemical environments. Because of the chalcophile affinity, Ge is commonly rich in several types of (Cu)–Pb–Zn deposits, including 'Kipushi-' or 'Tsumeb'-type (Chetty and Frimmel, 2000; Kampunzu et al., 2009; Melcher et al., 2006), Mississippi Valley-type (MVT) (Bernstein, 1985; Slack et al., 2004), and some metamorphosed ZnS deposits (Belissont et al., 2014). MVT deposits are expected to be the most important hosts of Ge-rich sphalerite, which was equally important to brown and hard coals (Frenzel et al., 2014).

Germanium has five naturally occurring stable isotopes, ^{70}Ge (20.84%), ^{72}Ge (27.54%), ^{73}Ge (7.73%), ^{74}Ge (36.28%), and ^{76}Ge (7.61%) (Rosman and Taylor, 1998). The early attempts made on using electron bombardment ion source mass spectrometry (Reynolds, 1953), thermal ionization mass spectrometry (TIMS) (Shima, 1963), solid source mass spectrometry (Green et al., 1986), secondary ionization mass spectrometry (SIMS) (Nishimura et al., 1988; Richter et al., 1999), and gas isotope mass spectrometry (GIMS) (Kipphardt et al., 1999) to analyze Ge isotopic compositions have been proved problematic due to the low precision of these techniques. Hirata (1997) has been a pioneer in the development of Ge isotopic measurements by multiple collector inductively coupled plasma-mass spectrometry (MC-ICP-MS). The improvement of mass discrimination and isobaric interference corrections and the establishment of suitable chemical preparation methods for various types of extraterrestrial and terrestrial samples make it possible to precisely determine Ge isotopes (with an analytical reproducibility of about ±0.2‰ and a minimum Ge quantity of ~15 ng) (Belissont et al., 2014; Escoube et al., 2008, 2012a,b; Galy et al., 2003; Luais, 2007, 2012; Luais et al., 2000; Qi et al., 2011; Rouxel et al., 2006, 2008; Siebert et al., 2006; Yang and Meija, 2010; Yang et al., 2011). Methods used to correct mass discrimination include double spikes (Escoube et al., 2012b; Siebert et al., 2006), external Ga isotope normalization (Galy et al., 2003; Luais, 2007, 2012), and sample-standard bracketing (SSB) (Escoube et al., 2008, 2012a,b; Qi et al., 2011; Rouxel et al., 2006, 2008). Comparison of these mass discrimination correction

* Corresponding author. Tel.: +86 13765051973; fax: +86 851 5891664.
E-mail address: qihuawen@vip.gyig.ac.cn (H.-W. Qi).

http://dx.doi.org/10.1016/j.oregeorev.2014.04.008
0169-1368/

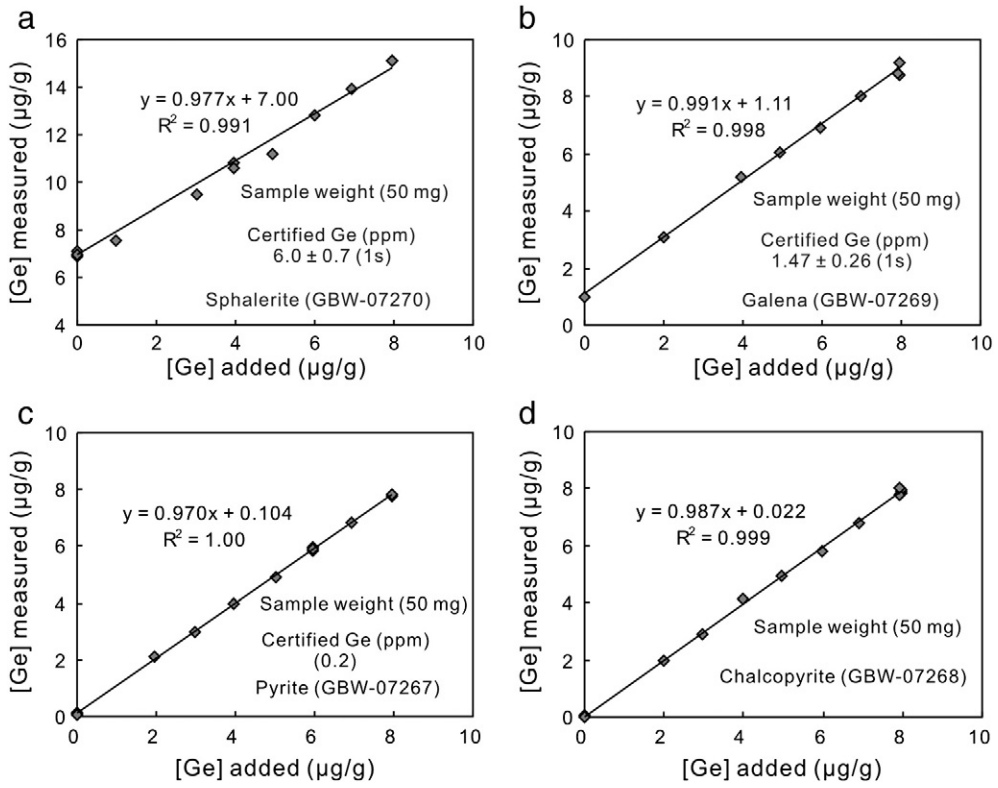

Fig. 1. Scatter diagrams of $[Ge]_{added}$ vs. $[Ge]_{measured}$ for synthetic samples. The synthetic samples were obtained by doping sulfides of CRMC with various amounts of Spex standard solution.

methods yielded a similar reproducibility of ±0.1‰ (2s) for δ^{74}Ge (Luais, 2012).

Different chemical preparation methods have been established for various types of samples, including 1) two-step separate technique for silicates using both the anion- and cation-exchange resins (Luais, 2012; Rouxel et al., 2006), 2) one step cationic-exchange method for Fe–Ni (iron meteorite and terrestrial iron formation) and ZnS matrices (Luais, 2007, 2012; Luais et al., 2000), 3) one step anion-exchange process of separating Ge from silicate and lignite matrices (Qi et al., 2011), and 4) the Mg-coprecipitation method for the pre-concentration of Ge from seawater (Escoube et al., 2008). Two-step separate technique for sphalerite can purify the Ge from the matrices effectively (Luais, 2012), but the process is complex and time-consuming. Moreover, the separation of Ge from the other sulfides except sphalerite was not reported. Single step anion-exchange technique was previously reported and used for separation of Ge in silicate (Escoube et al., 2012b; Qi et al., 2011), but for sulfides was rarely reported.

Recent studies have shown that distinct Ge isotopes fractionate during nebular condensation processes of planetary evolution, thermal fluid migration, and water–rock reactions (Escoube et al., 2008, 2012b; Luais, 2007, 2012; Qi et al., 2011; Rouxel et al., 2006, 2008; Siebert et al., 2006). Theoretical calculation showed that the Ge-bearing sulfides (e.g. sphalerite) can extremely enrich light Ge isotopes (more than 10‰ at 25 °C) compared with 4-coordinated Ge–O compounds (e.g. $Ge(OH)_{4(aq)}$ or quartz) (Li et al., 2009). The relative enrichment of light Ge isotopes in sphalerite has been proved by the Ge isotopic compositions of natural sphalerite samples from various geological settings. For example, sphalerite separates from the Navan Pb–Zn deposit, seafloor sulfide system (Escoube et al., 2012b), and Saint Salvy ZnS deposit, are rich in light Ge isotopes with δ^{74}Ge values ranging from −4.28‰ to 0.91‰ (Belissont et al., 2014; Luais, 2007, 2012). However, the fractionation mechanism of Ge isotopes and its controlling factors for natural sulfides from Pb–Zn deposits remain unclear. Moreover, in addition to sphalerite, the Ge isotopic compositions of other sulfides such as galena, pyrite, and chalcopyrite are not well known. Germanium isotopes may provide useful information for tracing Pb–Zn ore-forming processes.

In this study, a single step anion-exchange technique for sulfides was evaluated. The recoveries of Ge in four types of sulfides (sphalerite, galena, pyrite, and chalcopyrite) of certified reference materials of China (CRMC) (RGSMRM, 1995, for major and some trace elements) were quantitatively assessed. We demonstrate the reliable separation and purification of Ge from sulfide matrices and high-precision determination of Ge by HG-MC-ICP-MS. The Ge isotopic compositions of sphalerite, galena, and pyrite from the Jinding, Shanshulin, and Tianqiao Pb–Zn deposits in SW China were analyzed. The large Ge isotope fractionations of these sulfides indicate that Ge isotopes can be potential tracers of Pb–Zn ore-forming system.

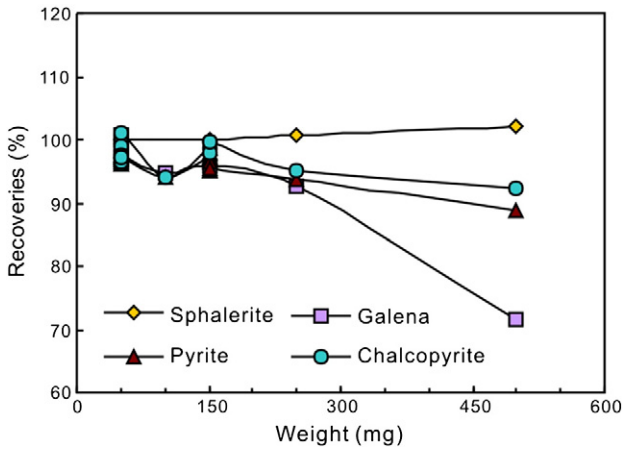

Fig. 2. Covariation diagram of Ge recovery with sample weights for different sulfides of CRMC.

Table 1
Trace element quantities of Ge, Cu, Zn, Sn, Sb, and Pb eluted from AG1-X8 anion exchange column for different sulfides of CRMC.

Sample	Volume	Sphalerite (GBW-07270) 100 mg + 400 ng Ge						Galena (GBW-07269) 100 mg + 400 ng Ge					
Eluant	(ml)	Ge (ng)	Cu (ng)	Zn (ng)	Sn (ng)	Sb (ng)	Pb (ng)	Ge (ng)	Cu (ng)	Zn (ng)	Sn (ng)	Sb (ng)	Pb (ng)
Filtrate	15	–	47,606	16,132,987		23,771	7291	–	5468	1568		30,255	1,174,342
1 M HF-2	2	–	2605	5,81,672	–	617	760	–	81.6	65.0	2.08	3074	34,685
1 M HF-4	2	–	60.8	28,805	8.85	54.8	228	–	11.5	–	3.92	3773	2436
1 M HF-6	2	–	24.0	8853	4.97	77.0	158	–	6.96	–	10.7	4178	136
1 M HF-8	2	–	10.0	2768	10.3	88.1	126	–	5.57	–	2.29	4192	25.4
1 M HF-10	2	–	10.6	162	13.0	98.4	128	–	10.6	162	1.98	98.4	128
H_2O	2	–	2.95	–	67.6	3.30	80.4	–	3.89	–	1.57	2763	13.0
3 M HNO_3 -2	2	345	20.6	39.1	59.8	1202	105	173	1.51	–	3643	14,677	21.3
3 M HNO_3 -4	2	123	4.11	–	22.8	1540	5.62	45.6	0.84	–	1129	7932	10.6
3 M HNO_3 -6	2	8.03	1.56	20.2	–	474	7.14	2.96	2.49	38.1	372	3300	10.5
3 M HNO_3 -8	2	–	2.94	23.2	64.3	284	3.19	–	1.75	–	29.7	2525	6.99
3 M HNO_3 -10	2	–	7.87	29.5	–	503	5.08	–	11.6	5.88	–	2984	9.17
3 M HNO_3 -12	2	–	2.31	–	72.4	693	2.53	–	1.00	–	4.19	3484	4.49
3 M HNO_3 -14	2	–	2.67	–	60.0	664	4.12	–	2.78	–	–	3820	2.83
3 M HNO_3 -16	2	–	3.64	–	–	897	4.25	–	1.74	–	–	3609	7.05
3 M HNO_3 -18	2	–	1.91	–	–	849	3.53	–	8.40	–	–	3221	7.61
3 M HNO_3 -20	2	–	82.2	894	64.3	679	517	–	1.07	–	18.6	2585	4.37
3 M HNO_3 -22	2	–	1.67	–	–	540	9.89	–	2.22	–	–	1964	684
3 M HNO_3 -24	2	–	2.48	–	–	342	6.68	–	1.86	–	10.1	1189	9.01
3 M HNO_3 -26	2	–	0.93	–	101	185	3.77	–	4.14	–	–	964	4.63
3 M HNO_3 -28	2	–	1.59	–	18.4	123	4.68	–	1.33	–	6.92	608	6.01
3 M HNO_3 -30	2	–	1.42	–	–	90.4	1.96	–	0.83	–	–	435	0.86
H_2O	10	–	2.98	150	–	34.9	7.00	–	1.02	46.3	–	138	64.4
3 M HNO_3	10	–	4.91	–	1.58	72.9	5.26	–	14.7	–	–	354	109
upload (ng)		471	42,771	26,590,997		10,650	42,344	214	2674	22,843	47,143	184,286	36,111,429
Recovery 1 (%)		0.00	6.34	2.34		8.81	3.50	0.00	4.49	3.58	0.05	9.81	0.10
Recovery 2 (%)		101	0.09	0.00		44.1	0.30	103	0.72	0.19	11.0	18.9	0.00

Sample	Volume	Pyrite (GBW-07267) 150 mg + 400 ng Ge						Chalcopyrite (GBW-07268) 150 mg + 400 ng Ge					
Eluant	(ml)	Ge (ng)	Cu (ng)	Zn (ng)	Sn (ng)	Sb (ng)	Pb (ng)	Ge (ng)	Cu (ng)	Zn (ng)	Sn (ng)	Sb (ng)	Pb (ng)
Filtrate	15	–	30,738	7625		20,456	2231	–	12,456,089	182,342		17,542	5043
1 M HF-2	2	–	1147	655	3.27	171	70.0	–	484,247	7239	–	806	476
1 M HF-4	2	–	33.6	24.2	2.18	201	40.2	–	22,961	332	–	91.3	300
1 M HF-6	2	–	8.52	–	7.75	269	28.5	–	1196	–	7.70	108	262
1 M HF-8	2	–	18.7	–	12.7	387	17.6	–	79.5	–	2.46	122	103
1 M HF-10	2	–	11.0	–	21.9	538	136	–	130	–	1520	158	68.3
H_2O	2	–	3.05	–	14.9	92.5	2.56	–	43.3	–	188	61.0	2375
3 M HNO_3 -2	2	157	25.2	–	57.3	8.82	3.42	140	23.4	–	240	5.46	4.54
3 M HNO_3 -4	2	31.7	2.93	–	68.7	6.54	3.06	34.9	7.15	–	49.9	5.91	5.06
3 M HNO_3 -6	2	2.83	1.51	–	–	4.37	4.54	1.73	9.02	–	–	2.54	5.44
3 M HNO_3 -8	2	–	1.39	–	–	3.99	4.65	–	1.29	–	3.91	2.17	2.72
3 M HNO_3 -10	2	–	2.18	–	38.3	4.30	4.86	–	4.07	–	5.70	2.62	4.96
3 M HNO_3 -12	2	–	1.11	–	–	4.06	1.24	–	80.8	–	97.1	1.80	9.75
3 M HNO_3 -14	2	–	1.60	–	–	4.18	1.16	–	30.0	–	112	2.87	4.78
3 M HNO_3 -16	2	–	0.60	–	–	3.59	1.78	–	2.71	–	–	3.39	4.85
3 M HNO_3 -18	2	–	1.11	–	–	3.65	8.67	–	2.22	–	–	3.06	4.61
3 M HNO_3 -20	2	–	6.93	–	–	3.11	11.1	–	1.61	–	–	2.96	5.68
3 M HNO_3 -22	2	–	0.99	–	–	2.88	5.18	–	1.82	–	10.0	2.34	3.51
3 M HNO_3 -24	2	–	0.78	–	–	2.57	4.64	–	2.88	18.7	157	1.18	36.0
3 M HNO_3 -26	2	–	3.17	23.7	–	2.50	0.55	–	7.12	–	–	1.48	5.75
3 M HNO_3 -28	2	–	1.17	–	8.49	1.76	3.24	–	4.94	–	–	1.12	11.1
3 M HNO_3 -30	2	–	2.70	–	–	2.03	1.58	–	1.36	–	–	0.94	2.74
H_2O	10	–	2.65	–	–	2.57	7.38	–	11.7	–	11.4	1.25	6.42
3 M HNO_3	10	–	2.13	–	–	2.06	4.84	–	2.34	–	–	1.19	4.12
upload (ng)		176	27,689	14,069		70.7	1503	171	21,435,686	193,114		174	8240
Recovery 1 (%)		0.00	4.41	4.83			19.6	0.00	2.37	3.92			43.5
Recovery 2 (%)		109	0.12	0.00		45.4	1.45	103	0.00	0.00		11.8	0.39

Notes: 400 ng Spex Ge was added to the powder sample before digestion. The quantity of elements illustrated above was based on 15 ml out of 35 ml sample solutions loaded on the anion-exchange chromatographic column. The calculated upload quantities of elements were based on sample weight, the certified or reference concentration of these elements, and the volume proportion of upload solution. The upload quantity of Pb includes the proportion of Pb-bearing precipitate; filtrate represents 15 ml sample solution passed the column, the quantity data of some elements less than several thousands nanograms of filtrate only listed for reference for the large dilution factor (2000) of this sample; Recovery 1 represents that of 10 ml 1 M HF and 2 ml of H_2O, while Recovery 2 represents that of 12 ml 3 M HNO_3 after H_2O elution. The element concentrations were determined by ICP-MS. "–" denotes below detection limit.

2. Experimental procedures

2.1. Reagents, certified reference materials, and natural samples

During chemical dissolution and purification, sub-boiling bi-distilled HNO_3 (treated by distillation in PFA equipment), trace metal grade HF and Milli-Q water (18.2 MΩ cm; Millipore, Billerica, MA, USA) were used. In order to reduce the Cl^+-based interference and avoid the formation of highly volatile $GeClO_4$, neither HCl and $HClO_4$ were used (Luais, 2012; Rouxel et al., 2006). The hydride generation (HG) agent was prepared before each analytical session and was composed of 8 g sodium borohydride powder (high purity $NaBH_4$; Fisher Chemical) and 4 g sodium hydride pellets (Analytical grade NaOH; Acros Organics, Thermo Fisher Scientific) dissolved in 1 L Milli-Q water.

Germanium standard solutions, NIST SRM 3120a ([Ge] = 1000 mg/l), Merck (1.70320.0100, [Ge] = 1000 mg/l), and Spex (CLGE9-1AY, [Ge] =

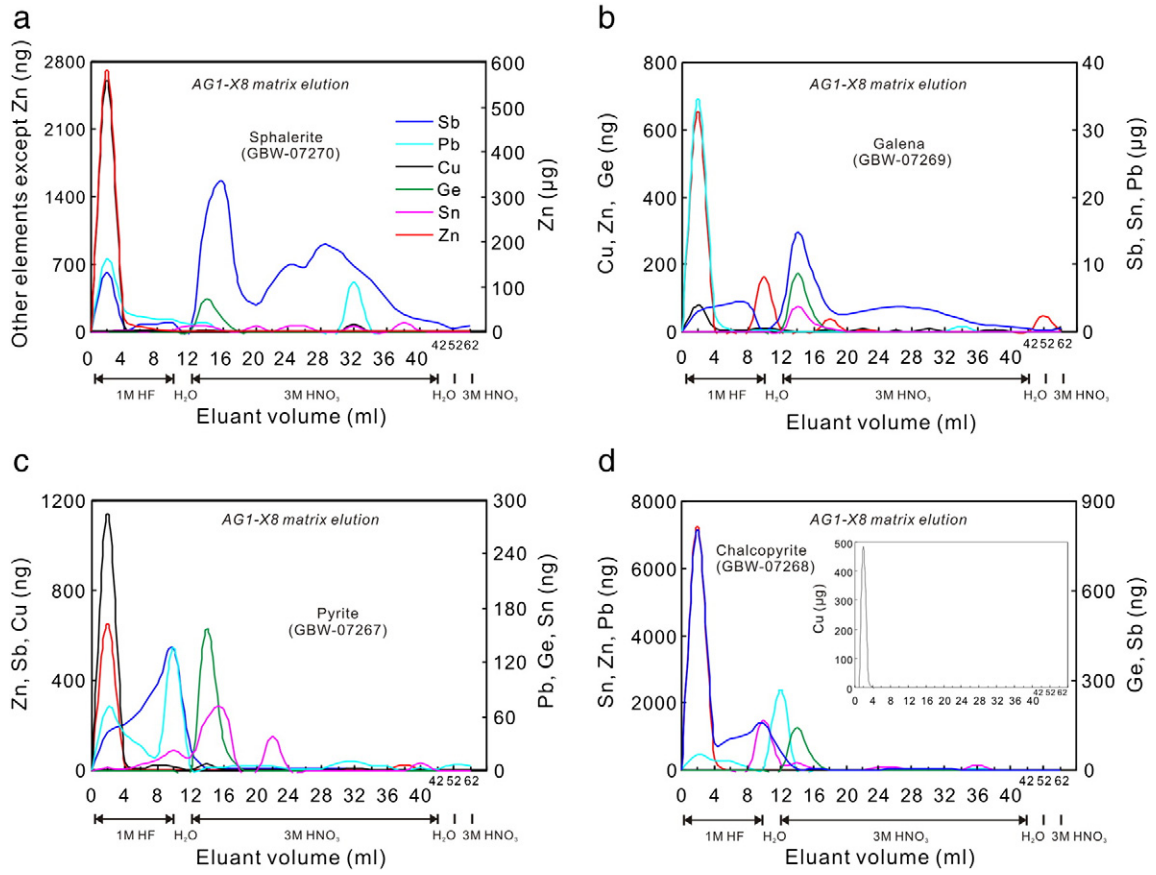

Fig. 3. The complete AG1-X8 elution scheme of Cu, Sb, Pb, Zn, Sn, and Ge of different sulfides of CRMC. 100, 100, 150, and 150 mg of sphalerite, galena, pyrite, and chalcopyrite of CRMC were weighted and doped with 400 ng of Spex Ge, respectively. The quantity of elements illustrated in figures was calculated based on 15 ml out of 35 ml sample solutions loaded on the anion-exchange chromatographic column.

10 μg/ml $(NH4)_2GeF_6$ in H_2O/tr HF) were prepared freshly before the analysis. Single element standard solutions of Zn (GSB 04-1761-2004), Sb (GSB 04-1748-2004), Pb (GSB 04-1742-2004), Cu (GSB 04-1725-2004), Sn (GSB 04-1753-2004), and W (GSB 04-1760-2004) of National Standard sample of China were used for matrix element doping experiments.

Four sulfides of CRMC (GBW-07270 sphalerite, GBW-07269 galena, GBW-07267 pyrite, and GBW-07268 chalcopyrite; Appendix A) (RGSMRM, 1995) with certified major elements Pb, Zn and S and some trace elements were used to evaluate the recoveries of Ge from different matrices during the whole separation and purification processes. Nature sulfide separates (sphalerite, galena, and pyrite) with sizes of 20 to 60 mesh were obtained by crushing the Pb–Zn ores from the Jinding, Shanshulin and Tianqiao Pb–Zn deposits in southwestern China and handpicking under a binocular microscope.

All Teflon beakers/vials used in this study were heated to 120 °C in 50% (V/V) concentrated guaranteed grade HNO_3, whereas plastic tubes and wares were treated with cool HCl (10%, V/V) for ~24 h. These containers were triply rinsed with Milli-Q water prior to sample collection. All cleaning and sample preparations were conducted in an ultraclean laboratory of the Institute of Geochemistry, Chinese Academy of Sciences.

2.2. Sample dissolution and chemical purification

Fifty to 150 mg of sulfides (sphalerite, galena, pyrite, and chalcopyrite) was dissolved with 10 ml of concentrated HNO_3 in a closed Teflon beaker on a hot plate at 120 °C overnight. Subsequently, the vessels were opened and sample solutions were dried at the same condition. The residues were digested using 1 ml of concentrated HF and 5 ml of Milli-Q water in the sealed PTFE containers on a hot plate at 120 °C overnight. The solutions with possible precipitates were transferred into 50 ml plastic centrifuge tubes and were conditioned to ~1 M HF. After centrifuged, 15 ml out of the 35 ml Ge-bearing supernatants was loaded on an anion-exchange chromatographic column filled with 1.2 ml (wet volume) AG1-X8 resin (Bio-Rad, Hercules, USA; 100–200 mesh; chloride form; cat # 140-1441). The column was previously washed using 10 ml of 3 M HNO_3 and 10 ml of Milli-Q water, and was then conditioned with 1 M HF. After adsorption of Ge on the column, 10 ml of 1 M HF and 2 ml of Milli-Q water were successively passed through the column to elute the remaining matrices. Germanium was then eluted with 12 ml of 3 M HNO_3, and the eluant was collected and taken to dryness on a hot plate at 80 °C. After evaporation, the solid residue was re-dissolved in 3–5 ml of 0.28 M HNO_3 for more than 2 h prior to Ge content and isotope analyses because HNO_3 can serve as a reaction media to suppress the yields of Se and As hydride formations (Rouxel et al., 2006).

2.3. Measurement of Ge concentration and isotopes

Germanium concentrations were determined using an ELAN DRC-e ICP-MS in the State Key Laboratory of Ore Deposit Geochemistry, Institute of Geochemistry, Chinese Academy of Sciences (CAS). A series of Merck standard solutions with different concentrations (0.1, 0.5, 1, 5, 10 and 100 ppb) were used to calibrate Ge concentrations in the final solution of various sulfide samples. Background counts for Ge in 0.28 M HNO_3 solutions are normally <50 cps (counts per second). Rhodium

Table 2
Germanium and matrix element contents and Ge isotopic compositions of composite samples doped with various amounts of matrix elements.

Sample no.	Ge (ppb)	Cu (ppb)	Cu/Ge	δ^{74}Ge ‰	2s	δ^{73}Ge ‰	2s	δ^{72}Ge ‰	2s	$\delta^{74/72}$Ge ‰	2s
Spex-Cu-1	20	80	4	−0.60	0.55	−0.22	0.66	−0.27	0.57	−0.33	0.28
Spex-Cu-2	20	120	6	−0.67	0.24	0.13	0.50	0.04	0.30	−0.71	0.54
Spex-Cu-3	20	160	8	−0.60	0.17	−0.59	0.04	−0.35	0.19	−0.25	0.02
Spex-Cu-4	20	240	12	−0.67	0.10	−0.36	0.71	−0.25	0.32	−0.43	0.42
Spex-Cu-5	20	320	16	−0.62	0.00	−0.50	0.07	−0.32	0.03	−0.30	0.03
Spex-Cu-6	20	400	20	−0.67	0.28	−0.52	0.04	−0.41	0.04	−0.26	0.64
	Ge (ppb)	Sn (ppb)	Sn/Ge	δ^{74}Ge ‰	2s	δ^{73}Ge ‰	2s	δ^{72}Ge ‰	2s	$\delta^{74/72}$Ge ‰	2s
Spex-Sn-1	20	200	10	−0.49	0.32	−0.33	1.12	−0.19	0.76	−0.30	0.06
Spex-Sn-2	20	400	20	−0.52	0.25	−0.44	1.00	−0.25	0.68	−0.27	0.40
Spex-Sn-3	20	600	30	−0.68	0.25	−0.74	0.45	−0.51	0.03	−0.16	0.22
Spex-Sn-4	20	800	40	−0.61	0.22	−0.56	0.65	−0.46	0.53	−0.15	0.32
Spex-Sn-5	20	1000	50	−0.60	0.20	−0.43	0.04	−0.30	0.12	−0.29	0.08
Spex-Sn-6	20	1200	60	−0.59	0.49	−0.84	0.40	−0.50	0.10	−0.08	0.39
	Ge (ppb)	W (ppb)	W/Ge	δ^{74}Ge ‰	2s	δ^{73}Ge ‰	2s	δ^{72}Ge ‰	2s	$\delta^{74/72}$Ge ‰	2s
Spex-W-1	20	400	20	−0.71	0.15	−0.45	0.50	−0.27	0.35	−0.43	0.20
Spex-W-2	20	800	40	−0.69	0.03	−0.53	0.00	−0.41	0.02	−0.28	0.06
Spex-W-3	20	1200	60	−0.63	0.44	−0.64	0.55	−0.35	0.30	−0.28	0.13
Spex-W-4	20	1600	80	−0.60	0.04	0.07	1.01	−0.13	0.50	−0.47	0.46
Spex-W-5	20	2000	100	−0.59	0.37	−0.44	0.15	−0.30	0.19	−0.29	0.18
Spex-W-6	20	3000	150	−0.55	0.00	−1.13	0.06	−0.71	0.13	0.16	0.13
	Ge (ppb)	Zn (ppb)	Zn/Ge	δ^{74}Ge ‰	2s	δ^{73}Ge ‰	2s	δ^{72}Ge ‰	2s	$\delta^{74/72}$Ge ‰	2s
Spex-Zn-1	20	100	5	−1.01	0.13	−1.06	0.40	−0.78	0.24	−0.22	0.11
Spex-Zn-2	20	200	10	−1.07	0.35	−0.80	1.43	−0.73	0.91	−0.35	0.16
Spex-Zn-3	20	300	15	−1.48	0.27	−1.79	0.70	−1.09	0.39	−0.39	0.67
Spex-Zn-4	20	400	20	−1.53	0.31	−1.36	0.02	−0.87	0.06	−0.65	0.37
Spex-Zn-5	20	600	30	−1.67	0.17	−1.15	0.48	−0.81	0.44	−0.86	0.26
Spex-Zn-6	20	1000	50	−1.95	0.28	−1.02	0.27	−0.76	6.14	−1.19	0.06
	Ge (ppb)	Pb (ppb)	Pb/Ge	δ^{74}Ge ‰	2s	δ^{73}Ge ‰	2s	δ^{72}Ge ‰	2s	$\delta^{74/72}$Ge ‰	2s
Spex-Pb-1	20	200	10	−0.84	0.13	−0.98	0.76	−0.54	0.34	−0.31	0.21
Spex-Pb-2	20	400	20	−1.05	0.05	−0.85	0.11	−0.60	0.03	−0.45	0.02
Spex-Pb-3	20	600	30	−1.11	0.30	−1.74	0.53	−1.03	0.38	−0.08	0.22
Spex-Pb-4	20	800	40	−1.10	0.00	−1.17	0.49	−0.72	0.32	−0.39	0.32
Spex-Pb-5	20	1000	50	−1.32	0.01	−1.49	0.16	−0.99	0.07	−0.33	0.08
Spex-Pb-6	20	1200	60	−1.33	0.01	−1.04	0.16	−0.69	0.07	−0.64	0.08
	Ge (ppb)	Sb (ppb)	Sb/Ge	δ^{74}Ge ‰	2s	δ^{73}Ge ‰	2s	δ^{72}Ge ‰	2s	$\delta^{74/72}$Ge ‰	2s
Spex-Sb-1	20	200	10	−0.72	0.04	−0.50	0.31	−0.35	0.01	−0.37	0.03
Spex-Sb-2	20	400	20	−0.78	0.39	−0.65	0.31	−0.38	0.20	−0.40	0.19
Spex-Sb-4	20	800	40	−0.81	0.20	−0.49	0.90	−0.39	0.51	−0.42	0.19
Spex-Sb-5	20	1000	50	−0.94	0.09	−0.89	0.58	−0.50	0.33	−0.44	0.24
Spex-Sb-6	20	1200	60	−1.12	0.11	−0.76	0.18	−0.53	0.09	−0.60	0.02
	Ge (ppb)	Zn (ppb)	Pb (ppb)	δ^{74}Ge ‰	2s	δ^{73}Ge ‰	2s	δ^{72}Ge ‰	2s	$\delta^{74/72}$Ge ‰	2s
Spex-S-1	20	22	8	−0.72	0.23	−0.55	0.18	−0.36	0.26	−0.32	0.11
Spex-S-2	20	14	300	−0.63	0.29	−0.51	0.32	−0.39	0.33	−0.38	0.17
Spex-H-1	20	148	46	−0.73	0.22	−0.60	0.28	−0.47	0.21	−0.37	0.01

Note: Sample number ended with "S-1" means that the sample was also doped with 4 ppb Cu, 6 ppb Sn, and 64 ppb Sb; sample number ended with "S-2" means that the sample was also doped with 4 ppb Cu, 302 ppb Sn, and 3280 ppb Sb; sample number ended with "H-1" means that the sample was also doped with 90 ppb Cu, 90 ppb Sn, 180 ppb Sb, and 182 ppb W simultaneously; "2s" denotes two times standard deviation.

was used as an internal standard for trace elements (Qi et al., 2000). The precision is usually better than ±8%.

Germanium isotope analyses were performed on a Nu-plasma high resolution (HR) MC-ICP-MS in the First Institute of Oceanography, State Oceanic Administration, China (SOA). The detailed operating conditions and parameters are similar to those described in Qi et al. (2011) and Rouxel et al. (2006). Sample solutions were introduced as hydrides through an on-line cold-vapor HG system (CETAC HGX-200), which minimizes argon and oxygen-based molecular ion matrix, and the interferences from alkalis (Escoube et al., 2012b; Rouxel et al., 2006, 2008). The Nu plasma instruments were operated at low mass resolution mode and on peak zero procedural blank correction. ^{68}Zn, ^{70}Ge, ^{72}Ge, ^{73}Ge and ^{74}Ge were measured on L4, L2, H2, H4 and H5 Faraday cups, whereas ^{69}Ga and ^{71}Ga were also monitored on L3 and Ax cups because of the interferences of ^{69}Ga^{1}H on ^{70}Ge and ^{71}Ga^{1}H on ^{72}Ge (Luais, 2012; Rouxel et al., 2006). High-purity argon gas was used for sample introduction. 0.28 M HNO_3 blank solutions were used for washing before each sample/standard measurement. The whole procedural blank of Ge was lower than 15 pg and indistinguishable from the instrumental blank. Samples and standard solutions were introduced by an autosampler (CETAC ASX-110FR) and a Minipuls 3 peristaltic pump (Gilson Corp., USA). Instrumental mass fractionations were corrected using the SSB method with NIST SRM 3120a Ge standard solution (e.g. Escoube et al., 2008, 2012a,b; Rouxel et al., 2006, 2008).

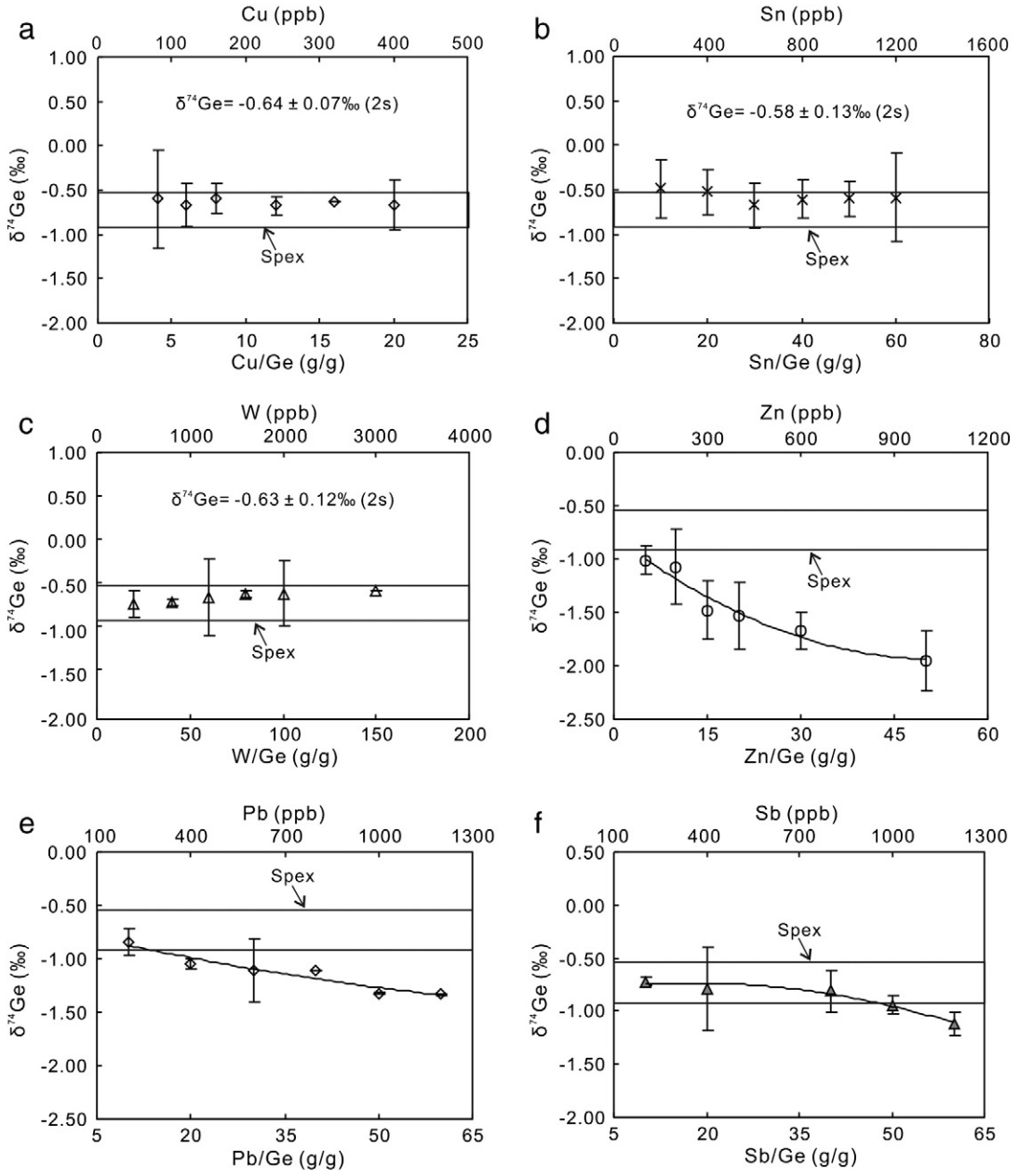

Fig. 4. Scatter diagrams of matrix element concentration or matrix element/Ge ratio vs. δ^{74}Ge value of synthetic samples doped with various amounts of (a) Cu, (b) Sn, (c) W, (d) Zn, (e) Pb, and (f) Sb.

Under normal conditions, about 3.5 ml of solution was analyzed at a concentration ranging from 5 to 50 ppb, which generate a total ^{74}Ge signal of 0.8 V_{mean} to 8.5 V_{mean}. Sometimes, the intensity dropped to half of these values. The Ge concentration of sample solutions and standard solutions was strictly matched (at the same concentration) before the measurement of the Ge isotopic compositions by the HG-MC-ICP-MS to preclude the possible matrix effects.

Introduction system were washed for different times (at least 4, 6, 7 and 8 min for 5, 10, 20 and 50 ppb solutions, respectively) between samples and standard solution measurements using 0.28 M HNO_3 until the signal intensity of ^{74}Ge decreased close to instrumental blank. Germanium isotope analysis comprised one block, which comprised 25 cycles with 4 s integration time per cycle. The standard errors for ^{74}Ge/^{70}Ge, ^{73}Ge/^{70}Ge, ^{72}Ge/^{70}Ge, and ^{74}Ge/^{72}Ge during 100 s continuing time are 0.00003, 0.00001, 0.00002, and 0.00002, respectively.

2.4. Data reduction

The variations in Ge isotopes are reported in terms of parts per mil deviations from an international standard and expressed in delta notation:

$$\delta^{X}\mathrm{Ge}(‰) = \left(\frac{\left({}^{X}\mathrm{Ge}/{}^{70}\mathrm{Ge}\right)_{\mathrm{Sample}}}{\left({}^{X}\mathrm{Ge}/{}^{70}\mathrm{Ge}\right)_{\mathrm{Standard}}} - 1\right) * 1000 \quad (1)$$

where X equals 74, 73, or 72. The standard isotopic values correspond to the average values of the NIST SRM 3120a, which has been recommended as international Ge isotope analysis standard because its Ge isotopic composition is closed to that of Bulk Silicate Earth (BSE) (Escoube et al., 2012b; Luais, 2012; Qi et al., 2011).

3. Evaluation of experimental results

3.1. Recovery of Ge after chemical digestion and purification

3.1.1. Standard-addition method

The standard-addition method has been used to evaluate the accuracy and precision of Mg, Ca, Ge and Fe isotope data in complex matrices (Rouxel et al., 2006, 2008; Tipper et al., 2008). In this study, we also used this method to investigate the recoveries of Ge during the whole chemical treatment by adding certain amounts of Ge standard solutions into several sulfides of CRMC.

Prior to sample dissolution and chemical purification, 50 mg sulfide powders of CRMC were doped with various amounts (0–400 ng) of Spex Ge. After the complete chemical purification scheme as described above, Ge concentrations of these composite samples were measured by ICP-MS. The measured Ge concentrations of the composite samples and the added amounts of Ge defined a straight line, whose regression coefficient is proportional to the yield of chemical purification (Fig. 1).

The quantitative recoveries of Ge from different sulfide matrices are 98 ± 5% (2s) (sphalerite), 99 ± 4% (2s) (galena), 97 ± 4% (2s) (pyrite), and 99 ± 4% (chalcopyrite) (2s) (Fig. 1). The calculated Ge concentration of sphalerite (7.00 ppm) is 16% higher than certified value (6.0 ± 0.7 ppm, 1 s) (RGSMRM, 1995). The calculated Ge concentration of galena (1.11 ppm) is slightly lower than the certified value (1.47 ± 0.26 ppm, 1 s) (RGSMRM, 1995). Pyrite and chalcopyrite of CRMC show lower Ge concentrations (0.104 and 0.022 ppm, respectively) than those of sphalerite and galena.

3.1.2. Correlation of Ge recovery with sample weight

For pure Ge-bearing solutions, the quantity of Ge for resin saturation can be calculated using the known capacity of milli-equivalent of the resin. However, for Ge-bearing solutions with large amount complex matrices, the resin will be saturated by matrices instead of by Ge. In order to evaluate the capacity of quantitative resin (1.2 ml wet volume), the relationship between Ge recovery and sample weight has been further assessed by dissolving various amounts of sulfides of CRMC (50 to 500 mg). Experimental results show that all sulfides weighing between 50 and 150 mg (only 15 ml out of the total 35 ml sample solution for resin separation) have good Ge recoveries (Fig. 2). The recoveries of Ge in galena, pyrite, and chalcopyrite decreased slightly when their weights were higher than 150 mg and decreased obviously when the sample weight reaches 500 mg (Fig. 2), especially for galena (only 71.4%). In summary, 1.2 ml of anion resin is enough for the purification of sphalerite, galena, pyrite, and chalcopyrite with weights lower than 150 mg. If larger amounts of samples were processed, larger volumes of resin were needed.

3.1.3. Elution curves of Ge and other matrix elements

The purpose of chemical purification is to separate Ge from other matrix elements. Most Ge was expectantly retained on the AG1-X8 anion exchange column while the majority of cations passed through. However, some residue matrix elements, such as Zn, Sb, Pb, Cu and Sn, on the column were eluted along with Ge as illustrated in Table 1 and Fig. 3. The leaching behaviors of these elements during uploading and elution processes were carefully checked.

For sphalerite, Zn and Cu have been completely eluted from the resin by 10 ml of 1 M HF and followed 2 ml of H_2O. However, most Sb and Pb remained on the resin after HF elution and were eluted again by 3 M HNO_3. A part of Sb was eluted by ~4 ml of 1 M HF, but Sb was continuously removed from the resin by using 2 to 40 ml of 3 M HNO_3 (Fig. 3a). Some Pb was also eluted at the HF stage, but Pb appeared again when the volume of 3 M HNO_3 reaches about 20 ml due to remained Pb on the column during the last elution (Fig. 3a). Nearly all the Ge was recovered by ~5 ml of 3 M HNO_3. There is no obvious trend of Sn during the whole elution process due to the low Sn contents in sphalerite. The recoveries of Ge, Cu, Zn, Sb, Pb in 12 ml 3 M HNO_3 after 2 ml H_2O are 101%, 0.09%, <0.0001%, 44.1%, and 0.30%, respectively.

With respect to galena, more than 96.64% of total Pb quantity were precipitated possibly as PbF_2 or $PbSO_4$ in 1 M HF media, the majority of Zn, and minor Pb, Cu, and Sb have been eluted by 10 ml of 1 M HF and followed 2 ml of H_2O (Fig. 3b). But remained Sb and Sn were eluted along with Ge by about 5 ml of 3 M HNO_3. Minor Pb appeared again when the volumes of 3 M HNO_3 reach 4 and 30 ml because minor Pb remained on the column during the last elution. High concentration Ag also was found in the eluant. The recoveries of Ge, Cu, Zn, Sn, Sb, Pb in 12 ml 3 M HNO_3 after 2 ml H_2O are 103%, 0.72%, 0.19%, 11.0%, 18.9%, and <0.0001%, respectively.

Table 3
The intensities of ^{68}Zn and Ge isotopes, and isotope ratios of composite samples doped with various amounts of Zn, Pb and Sb (monitored by HG-MC-ICP-MS).

				Intensity (volt) of isotopes monitored by MC-ICP-MS					Isotope ratios				
Sample no.	Zn/Ge	Ge (ppb)	Zn (ppb)	^{70}Ge	^{72}Ge	^{73}Ge	^{74}Ge	^{68}Zn	$^{74/70}Ge$	$^{73/70}Ge$	$^{72/70}Ge$	$^{74/72}Ge$	$^{68}Zn/^{70}Ge$
Spex-Zn-1	5	20	100	0.49585	0.69547	0.20066	0.97106	0.00002	1.95835	0.40468	1.40258	1.39625	0.00003
Spex-Zn-2	10	20	200	0.48856	0.68535	0.19783	0.95616	0.00000	1.95708	0.40491	1.40279	1.39513	0.00001
Spex-Zn-3	15	20	300	0.47075	0.66007	0.19039	0.92143	0.00003	1.95739	0.40445	1.40217	1.39597	0.00005
Spex-Zn-4	20	20	400	0.44861	0.62909	0.18147	0.87805	0.00000	1.95727	0.40453	1.40231	1.39575	0.00000
Spex-Zn-5	30	20	600	0.45470	0.63759	0.18395	0.88969	0.00001	1.95667	0.40455	1.40221	1.39541	0.00003
Spex-Zn-6	50	20	1000	0.43712	0.61287	0.17683	0.85501	0.00001	1.95599	0.40453	1.40206	1.39509	0.00003
	Pb/Ge	Ge (ppb)	Pb (ppb)	^{70}Ge	^{72}Ge	^{73}Ge	^{74}Ge	^{68}Zn	$^{74/70}Ge$	$^{73/70}Ge$	$^{72/70}Ge$	$^{74/72}Ge$	$^{68}Zn/^{70}Ge$
Spex-Pb-1	10	20	200	0.54427	0.76214	0.21963	1.06367	0.00002	1.95429	0.40353	1.40029	1.39563	0.00005
Spex-Pb-2	20	20	400	0.54866	0.76832	0.22148	1.07206	0.00002	1.95394	0.40368	1.40035	1.39533	0.00003
Spex-Pb-3	30	20	600	0.54959	0.76918	0.22161	1.07357	0.00001	1.95338	0.40323	1.39955	1.39572	0.00003
Spex-Pb-4	40	20	800	0.53291	0.74588	0.21493	1.04075	0.00002	1.95297	0.40331	1.39964	1.39534	0.00003
Spex-Pb-5	50	20	1000	0.52711	0.73750	0.21248	1.02922	0.00001	1.95255	0.40309	1.39913	1.39554	0.00003
Spex-Pb-6	60	20	1200	0.52246	0.73122	0.21070	1.02012	0.00001	1.95253	0.40327	1.39956	1.39511	0.00001
	Sb/Ge	Ge (ppb)	Sb (ppb)	^{70}Ge	^{72}Ge	^{73}Ge	^{74}Ge	^{68}Zn	$^{74/70}Ge$	$^{73/70}Ge$	$^{72/70}Ge$	$^{74/72}Ge$	$^{68}Zn/^{70}Ge$
Spex-Sb-1	10	20	200	0.56780	0.79496	0.22912	1.10934	0.00001	1.95374	0.40351	1.40007	1.39546	0.00002
Spex-Sb-2	20	20	400	0.55866	0.78208	0.22539	1.09127	0.00003	1.95337	0.40345	1.39992	1.39534	0.00005
Spex-Sb-4	40	20	800	0.50635	0.70766	0.20387	0.98641	0.00001	1.94807	0.40264	1.39756	1.39390	0.00003
Spex-Sb-5	50	20	1000	0.46327	0.64719	0.18636	0.90211	0.00006	1.94727	0.40226	1.39700	1.39389	0.00012
Spex-Sb-6	60	20	1200	0.42818	0.59810	0.17224	0.83364	0.00007	1.94694	0.40226	1.39685	1.39381	0.00016

For pyrite, nearly all the Cu, Pb, Zn, and Sb were removed by 10 ml of 1 M HF and 2 ml of H_2O, Ge was largely recovered from the resin using about 5 ml of 3 M HNO_3 (Fig. 3c). Sn was eluted along with Ge recovery, and appeared again when the volume of 3 M HNO_3 reach 8 ml due to remained Sn on the column during the last elution (Fig. 3c). The recoveries of Ge, Cu, Zn, Sb, Pb in 12 ml 3 M HNO_3 after 2 ml H_2O are 109%, 0.12%, 0.00%, 45.4%, and 1.45%, respectively.

For the elution scheme of chalcopyrite, nearly all the matrices were completely eluted from the resin by 10 ml of 1 M HF and 2 ml of H_2O (Fig. 3d). Minor remained Sb and Pb on the resin were eluted by HNO_3 at the beginning of Ge recovery and were completely removed using 2 ml of 3 M HNO_3 (Fig. 3d). The recoveries of Ge, Sb, and Pb in 12 ml 3 M HNO_3 are 103%, 11.8%, and 0.39%, respectively.

Significant Sb remained in the Ge-bearing solution and no obvious principles of Sb elution scheme for sphalerite and galena samples possibly result from the similar partition coefficient of Sb with Ge in acid medium (Fig. 3) (Lobo et al., 2013). Further work was needed to optimize Sb separation procedure.

3.1.4. Matrix effects

As mentioned above, after purification, several elements such as Zn, Sb, Cu, Sn, Pb, and possibly W, were remained in the final solution prepared for Ge isotopic composition analysis. The matrix effects of these elements were investigated by comparison of Ge isotopic composition of Spex standard solution and the doped 20 ppb Spex standard solution with one element or several matrix elements determined by HG-MC-ICP-MS. Matrix element/Ge concentration ratios (ppb/ppb) are defined according to the true ratios of the eluant after purification of natural sulfides from several Pb–Zn deposits in SW China. The δ^{74}Ge values of these composite samples are listed in Table 2.

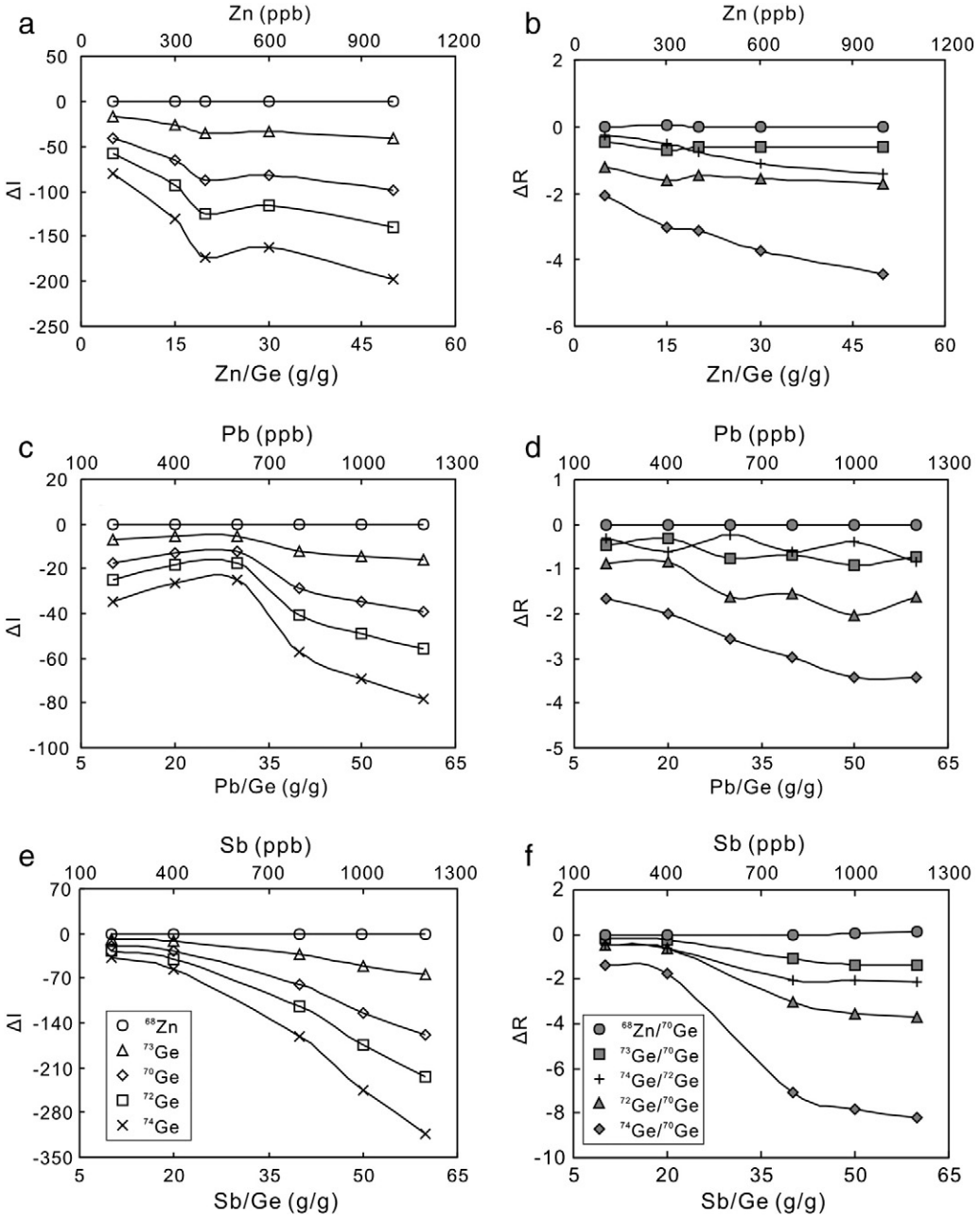

Fig. 5. The negative deviation values of intensity (ΔI) and isotope ratios (ΔR) of synthetic samples doped with various amounts of matrix elements, relative to those of NIST SRM 3120a. $\Delta I = (I_{sample} - I_{NIST}) * 1000$; $\Delta R = (R_{sample} - R_{NIST}) * 1000$.

For the composite samples doped with Cu, Sn, and W, with the increase of concentrations of these elements, even when the Cu/Ge, Sn/Ge, and W/Ge ratios of these samples is up to 20, 60, and 150, respectively, their Ge isotopic compositions are still constant with average δ^{74}Ge values of -0.64 ± 0.07‰ (2s, n = 6), -0.58 ± 0.13‰ (2s, n = 6), and -0.63 ± 0.12‰ (2s, n = 6), respectively. These values are indistinguishable from the δ^{74}Ge value of pure Spex standard solution (-0.70 ± 0.19‰; 2s, n = 27; Table 5) within analytical uncertainty (Fig. 4a–c). This indicates that high concentration of these elements does not produce significant bias on the Ge isotopic composition of samples determined by HG-MC-ICP-MS.

However, the Ge isotopic compositions of composite samples doped with Zn, Pb, and Sb are negatively correlated with the concentrations of doped elements (Fig. 4d–f). 1000 ppb Zn, 1200 ppb Pb, and 1200 ppb Sb mixing with 20 ppb Spex standard solutions produced negative shifts of about −1.3‰, −0.6‰, and −0.4‰ in δ^{74}Ge value, respectively. It is worth noting that the negative shift (−1.3‰) produced by 1000 ppb Zn determined by HG-MC-ICP-MS is distinctly smaller than that −27‰ shift in δ^{74}Ge induced by 800 ppb Zn without Zn interference corrections determined by PFA nebulizer-MC-ICP-MS (Luais, 2012). Therefore, the single anion resin purification method is only suitable to the samples injected by HG for Ge isotope measurement.

The ^{68}Zn intensities of composite samples doped with various amounts of Zn, Sb, and Pb are generally less than 0.00007 V, and their ^{68}Zn/^{70}Ge ratios are less than 0.16‰, indicating that Zn does not form hydride during analysis process. Moreover, white precipitate (possible $Zn(OH)_2$) that adhere to inner surface of HG was found during the analysis of solutions with high Zn concentration. Both the intensities of Ge isotopes and isotope ratios of these samples doped with Zn, Sb, and Pb decreased, and heavy Ge isotope (^{74}Ge) decreased much more quicker than that of light Ge isotope (^{70}Ge), with increasing concentration of doped elements (Zn, Pb, and Sb) (Table 3 and Fig. 5). These facts indicate that high Zn, Pb, and Sb in the final solution would suppress germane formation that fractionates Ge isotopes (Dedina et al., 1995). Therefore,

Table 4
Trace element concentrations (ppb) in the final Ge-bearing solutions of natural sulfides for Ge isotope analyses.

Deposits	Jinding Pb–Zn deposit					Shanshulin Pb–Zn deposit						Tianqiao Pb–Zn deposit				
Sample no.	JD-09-21	JD-09-63	JD-09-44	JD-09-58	JDJ-10-40	SSL-1	SSL-3	SSL-3	SSL-4	SSL-6	SSL-6	TQ-8	TQ-10	TQ-11	TQ-11	TQ-12-1
Mineral	Sp	Sp	Gn	Py	Py	Sp	Gn	Sp	Py	Py	Gn	Py	Sp	Py	Sp	Py
Li	–	–	–	–	–	–	0.062	–	0.061	0.026	0.038	0.048	–	0.043	–	0.20
Be	–	–	–	–	–	–	0.041	–	–	–	–	–	–	–	–	–
Sc	–	–	0.17	0.14	0.34	0.22	0.48	0.21	0.55	0.15	0.29	0.41	0.51	0.73	0.30	2.11
V	0.078	0.051	–	0.103	0.13	–	–	–	0.25	0.088	–	0.23	–	0.41	–	0.97
Cr	0.12	0.097	–	–	–	0.11	–	–	0.18	0.087	–	0.30	–	0.41	–	0.50
Co	–	–	0.049	0.026	0.098	0.010	–	–	0.015	–	–	0.29	–	–	–	0.024
Ni	–	–	–	–	–	–	–	–	–	–	–	–	–	–	–	–
Cu	1.65	1.33	2.96	14.4	18.1	0.77	0.24	0.81	7.77	1.88	0.17	5.59	1.93	9.56	1.08	25.1
Zn	9.70	7.90	22.1	24.4	23.4	6.98	1.68	6.33	10.2	2.83	0.15	18.1	2.50	21.1	7.88	33.6
Ga	–	–	–	–	–	–	–	–	–	–	–	0.004	–	0.005	–	0.021
Ge	10.0	10.0	5.00	5.00	5.00	50.0	5.00	50.0	5.00	5.00	5.00	20.0	50.0	5.00	50.0	5.00
As	7.51	2.02	267	544	1037	0.021	0.096	0.030	10.3	26.1	12.5	27.2	62.5	66.0	7.34	446
Rb	–	–	0.057	0.017	–	0.002	0.014	–	0.025	0.007	0.010	0.022	–	0.011	–	0.070
Sr	0.14	0.064	0.079	3.36	–	–	0.045	–	0.048	–	–	0.043	–	0.036	–	–
Y	0.036	–	0.005	1.07	–	–	0.005	–	0.009	–	–	0.003	–	0.007	–	0.067
Zr	1.97	7.16	2.91	5.06	11.0	0.048	0.28	0.031	0.75	0.79	0.36	0.97	1.23	2.44	0.16	11.3
Nb	0.17	0.28	4.05	0.133	0.17	–	–	–	0.004	0.007	–	0.013	0.004	0.049	0.002	0.086
Mo	16.1	3.41	96.0	427	125	0.014	0.10	0.006	0.77	0.26	0.21	0.26	0.18	0.99	0.023	2.11
Ag	0.13	0.063	32.9	15.9	0.99	0.006	0.072	–	0.032	0.020	0.079	0.035	–	0.083	–	0.18
Cd	0.45	0.16	5.79	1.08	0.23	0.017	0.59	0.195	0.080	0.033	–	0.81	0.21	0.10	0.11	0.64
In	–	–	–	–	–	–	–	–	–	–	–	–	–	–	–	–
Sn	1.06	1.14	7.76	2.89	1.86	0.046	0.14	0.100	0.33	0.39	0.30	1.79	6.63	1.87	1.97	3.14
Sb	2.21	7.68	113	14.4	6.88	1.13	85.9	0.67	23.7	17.1	241	31.8	7.76	30.0	6.68	236
Cs	–	–	–	–	–	–	–	–	–	–	–	–	–	–	–	–
Ba	0.92	0.66	0.41	15.0	0.20	–	1.39	–	1.36	0.39	0.81	1.06	–	1.90	–	4.65
La	0.038	–	–	0.75	–	–	0.023	–	0.007	0.003	0.038	0.006	–	0.008	–	0.052
Ce	0.077	–	0.045	1.97	0.026	–	3.91	–	4.30	1.11	2.73	2.91	–	5.00	–	14.0
Pr	–	–	–	0.27	–	–	–	–	–	–	–	–	–	–	–	–
Nd	0.046	–	–	1.24	–	–	–	–	–	–	–	–	–	–	–	–
Sm	–	–	–	0.22	–	–	–	–	–	–	–	–	–	–	–	–
Eu	–	–	–	0.053	–	–	–	–	–	–	–	–	–	–	–	–
Gd	–	–	–	0.22	–	–	–	–	0.030	0.007	0.020	0.015	–	0.040	–	0.12
Tb	–	–	–	–	–	–	–	–	–	–	–	–	–	–	–	–
Dy	–	–	–	0.15	–	–	–	–	–	–	–	–	–	–	–	–
Ho	–	–	–	–	–	–	–	–	–	–	–	–	–	–	–	–
Er	–	–	–	0.075	–	–	–	–	–	–	0.012	–	–	–	–	0.054
Tm	–	–	–	–	–	–	–	–	–	–	–	–	–	–	–	–
Yb	–	–	–	0.035	–	–	–	–	–	–	–	–	–	–	–	–
Lu	–	–	–	–	–	–	–	–	–	–	–	–	–	–	–	–
Hf	0.063	0.20	–	0.027	–	–	–	–	–	–	–	–	–	–	–	–
Ta	–	0.025	0.83	–	–	–	–	–	–	–	–	–	–	–	–	–
W	0.72	0.065	0.079	0.12	1.52	–	0.002	–	0.31	0.097	0.011	8.66	–	0.099	–	0.53
Tl	–	–	–	0.20	–	–	–	–	–	–	–	–	–	–	–	–
Pb	6.52	0.34	43.2	1127	2.28	0.16	32.0	1.51	1.13	0.539	11.349	7.79	0.17	7.56	0.24	7.99
Bi	–	–	–	–	–	–	–	–	–	0.000	–	0.004	–	0.003	–	0.006
Th	–	–	–	–	–	–	–	–	–	0.001	–	0.001	–	0.003	–	0.037
U	0.30	0.13	0.28	0.73	0.22	0.030	0.17	–	1.71	0.644	0.075	0.10	0.034	0.43	–	0.57

Note: Sp, sphalerite (ZnS); Py, pyrite (FeS_2); Gn, galena (PbS); –, below detection limit.

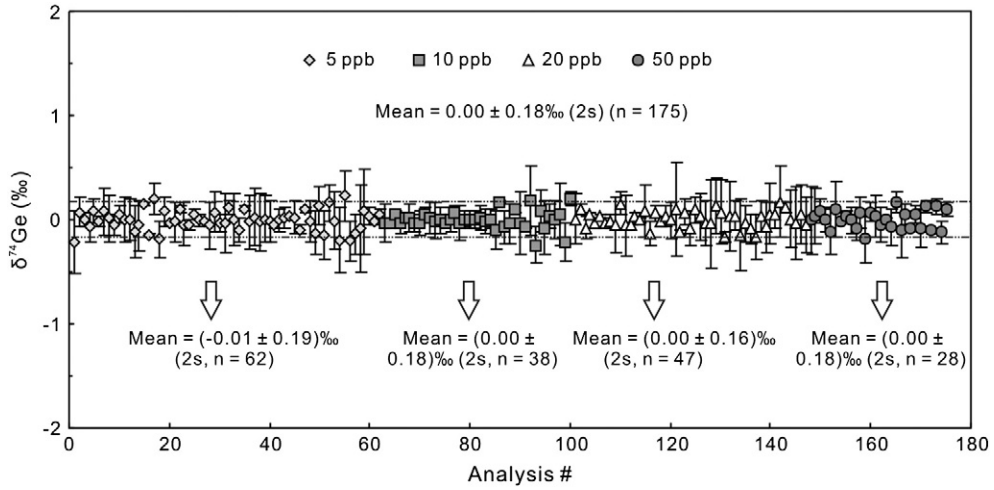

Fig. 6. Long-term reproducibility of Ge isotopic composition of NIST SRM 3120a during several analytical sessions (eight months) using SSB method. Uncertainties (error bar in the diagram) are the two times standard deviation at 95% confidence intervals.

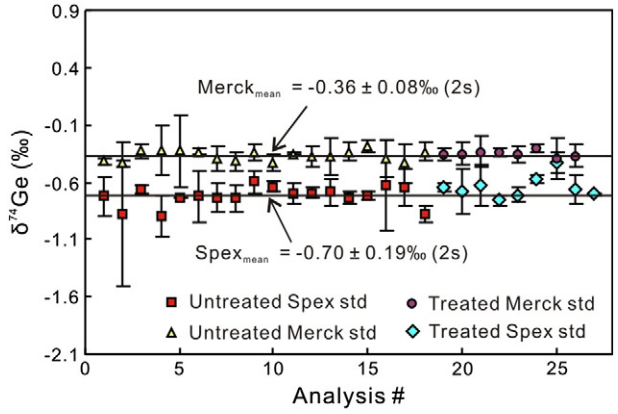

Fig. 7. Repeated analyses of Ge isotopic compositions of Merck and Spex standard solutions using SSB method. "Treated" means that the standard solution underwent the same dissolution and chemical purification processes as ordinary sample. "Untreated" means that the standard solution was prepared directly. Uncertainties (error bar in the diagram) are the two times standard deviation at 95% confidence intervals.

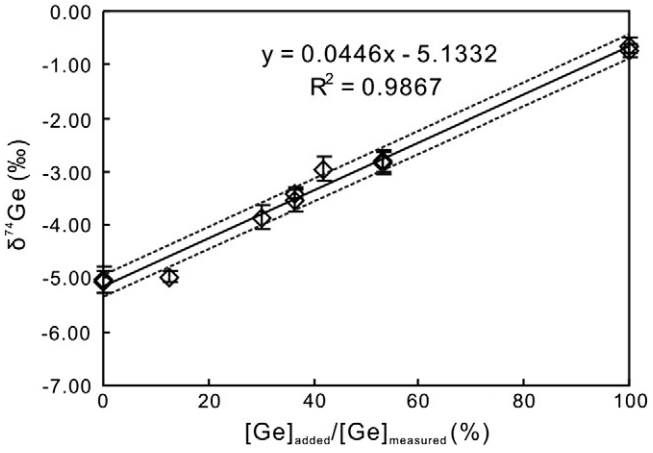

Fig. 8. Ge isotopic compositions of synthetic samples obtained by doping sphalerite (GBW-07270) with various amounts of pure Spex Ge standard solution. The two dashed lines denote the uncertainties (±0.19‰, 2s).

Table 5
Intercalibration of Ge isotopic composition of Spex Ge standard solution against NIST SRM 30120a.

Laboratory	Introduction system	Correction method	nb #	δ^{74}Ge ‰	2s	δ^{73}Ge ‰	2s	δ^{72}Ge ‰	2s	$\delta^{74/72}$Ge ‰	2s	References
WHOI	HG	SSB	1	−0.59	nd	nd		−0.28	nd	−0.31	nd	Escoube et al. (2012b)
WHOI	HG	Ga	1	−0.60	nd	nd		−0.28	nd	−0.31	nd	Escoube et al. (2012b)
WHOI	HG	SSB	5	−0.84	0.16	nd		−0.48	0.10	−0.36	0.08	Escoube et al. (2012b)
WHOI	HG	Ga	5	−0.81	0.11	nd		−0.46	0.09	−0.35	0.04	Escoube et al. (2012b)
IFREMER	SiS	SSB	3	−0.61	0.04	−0.51	0.09	−0.33	0.03	−0.28	0.05	Escoube et al. (2012b)
IFREMER	SiS	DS	4	−0.63	0.13	−0.48	0.10	−0.32	0.06	−0.31	0.06	Escoube et al. (2012b)
LCBIE	SiS	SSB	14	−0.64	0.42	nd		nd	0.00	−0.23	0.26	Escoube et al. (2012b)
LCBIE	SiS	Ga	14	−0.79	0.18	nd		nd	0.00	−0.31	0.04	Escoube et al. (2012b)
Average value				−0.69	0.21	−0.50	0.04	−0.36	0.18	−0.31	0.08	
CRPG	SiS	Ga	10	−0.81	0.19	−0.62	0.24	−0.41	0.11	nd		Luais (2012)
CRPG	SiS	SSB	10	−0.79	0.18	−0.62	0.16	−0.41	0.12	nd		Luais (2012)
WHOI	HG	SSB	9	−0.70	0.11	−0.51	0.16	−0.37	0.06	−0.34	0.06	Qi et al. (2011)
SOA	HG	SSB	27	−0.70	0.19	−0.57	0.23	−0.38	0.11	−0.33	0.12	This study
Average value				−0.72	0.16	−0.55	0.12	−0.38	0.10	−0.31	0.08	

Note: HG, hydride generation; SiS, cyclonic spray chamber; SSB, sample-standard bracketing; DS, double spike correction; Ga, external normalization to Ga; nd, not determined; "2s" denotes two times standard deviation.

Table 6
Ge isotopic compositions of sphalerite standard samples and composite samples doped with various amounts of Spex Ge standard solution.

Sample no.	Sample type	$Ge_{add}/Ge_{measured}$	Ge (ppb)	Zn (ppb)	Zn/Ge	δ^{74}Ge (‰)	2s	δ^{73}Ge (‰)	2s	δ^{72}Ge (‰)	2s	$\delta^{74/72}$Ge (‰)	2s
GeB1-04	Sp-std	0	20	23.3	1.16	−5.05	0.20	−3.89	0.18	−2.84	0.36	−2.21	0.07
GeB1-05	Sp-std	0	20	57.2	2.86	−5.01	0.25	−3.63	0.80	−2.78	0.56	−2.24	0.86
GeB2-04	Spex-Sp-std	13	20	192	9.58	−4.96	0.10	−3.68	0.03	−2.46	0.04	−2.51	0.06
GeB2-05	Spex-Sp-std	30	20	33.9	1.70	−3.86	0.23	−2.75	0.19	−1.96	0.05	−1.91	0.18
GeB2-06	Spex-Sp-std	36	20	23.2	1.16	−3.40	0.09	−2.75	0.27	−1.70	0.03	−1.70	0.06
GeB2-07	Spex-Sp-std	36	20	21.0	1.05	−3.54	0.20	−2.69	0.06	−1.71	0.13	−1.83	0.08
GeB2-08	Spex-Sp-std	42	20	10.2	0.51	−2.95	0.22	−2.33	0.36	−1.58	0.38	−1.37	0.54
GeB2-12	Spex-Sp-std	53	20	57.9	2.90	−2.84	0.19	−2.17	0.33	−1.37	0.28	−1.47	0.11
GeB2-13	Spex-Sp-std	53	20	10.0	0.50	−2.80	0.23	−2.25	0.50	−1.38	0.53	−1.42	0.39

Note: "2s" denotes two times standard deviation.

the concentrations of these elements in the final solution prepared for Ge isotope analysis by one step anion-exchange process should be carefully checked.

The matrix effects of multiple elements on the Ge isotopic compositions were also investigated by doping 20 ppb Spex Ge standard solutions with various amounts of Cu, Zn, Sb, Pb, Sn, and W simultaneously. The matrix element/Ge concentration ratios were also defined according to the average ratios in the final solutions of purified natural sulfide samples of this study. The composite samples, Spex-S-1, Spex-S-2, and Spex-H-1, simulate the average matrix compositions of sphalerite, galena, and pyrite samples after purification, respectively. The δ^{74}Ge values of these composite samples range from −0.63‰ to −0.73‰, indistinguishable from that (−0.70 ± 0.19‰) of Spex standard solution within analytical uncertainty.

The trace element concentrations in the final solutions of purified natural sulfides for Ge isotope analyses were presented in Table 4. The relatively high quantity (about 200 ng) of residual Sb in the final solutions of galena may be attributed to the existence of Sb as a major trace element or paragenetic Pb–Sb sulfosalts within galena (Li et al., 2005; Liu et al., 1984). Minor amounts of Zn, Pb, Cu, Sn, W, and As also remained for sphalerite and pyrite samples. As and Se also have less interference on Ge isotope measurement (Rouxel et al., 2006). The highest concentrations of Zn (33.6 ppb), Pb (with an exception of one sample (JD-09-58) which might be contaminated by former used resin, generally less than 43.2 ppb), and Sb (236 ppb) in the final solution of purified natural sulfide samples are distinctly lower than the concentration levels of these elements that can lead to significantly biases of Ge isotopic compositions. Therefore, single step anion resin purification method is suitable for Ge isotope analysis of natural sulfides determined by HG-MC-ICP-MS. If the sample introduction system was changed, more rigorous purification method should be developed and matrix effects should be re-evaluated.

3.2. Reproducibility and Ge isotopic composition of standard samples

Duplicate measurements of NIST SRM 3120a during 8-month analytical processes yielded an average δ^{74}Ge value of 0.00 ± 0.18‰ (2s, n = 175) (Fig. 6), indicating a long-term reproducibility of about ± 0.18‰. The precision values for Ge contents of 5 ppb, 10 ppb, 20 ppb, and 50 ppb are ±0.19‰, ±0.18‰, ±0.16‰, and ±0.18‰, respectively. There are no systematic variations between the precision and Ge concentration (Fig. 6).

Repeated analyses of Spex standard solutions yielded an average δ^{74}Ge value of −0.70 ± 0.19‰ (2s, n = 27) (Fig. 7), which is coincident with previously reported average values of −0.69 ± 0.21‰ (2s) (Escoube et al., 2012b) and −0.70 ± 0.11‰ (2s) (Qi et al., 2011) (Table 5). A complete comparison of these delta values with those of Escoube et al. (2012b), Luais (2012), and Qi et al. (2011) has been illustrated in Table 5. Merck standard solution was firstly certified in this study and yielded a mean δ^{74}Ge value of −0.36 ± 0.08‰ (2s, n = 26), which was similar to those of JMC Ge standard solution (−0.32 ± 0.10‰) (2s, n = 6) (Escoube et al., 2012b). The treated Spex (n = 8) and Merck (n = 8) Ge standard solutions, processed the same dissolution and one step anion-exchange chemical purification method as ordinary samples, yielded Ge recoveries of 94.8%–98.8% and 94.2%–100.0%, respectively. There are no differences in Ge isotopic composition between the treated and untreated Spex or Merck Ge standard solutions (Fig. 7).

The δ^{74}Ge values of the composite samples (sphalerite GBW-07270 doped with various amounts of Spex solution) and the percentage of Ge added in these composite samples strictly follow the predicted mixing line between sphalerite GBW-07270 and Spex standard solution, and the calculated δ^{74}Ge value of sphalerite GBW-07270 is −5.13‰, which is indistinguishable from the duplicate measured values (−5.05‰ and −5.01‰) of sphalerite GBW-07270 within analytical error (Fig. 8 and Table 6). These facts demonstrate that there is no Ge isotope fractionation during the whole purification and analysis process.

4. Applications of Ge isotope analyses of natural sulfides from Pb–Zn deposits

The Jinding, Shanshulin, and Tianqiao deposits in southwestern China are sediment-hosted Pb–Zn deposits (Fig. 9), which are important hosts of disperse elements, especially Ge and Cd. The Jinding deposit is

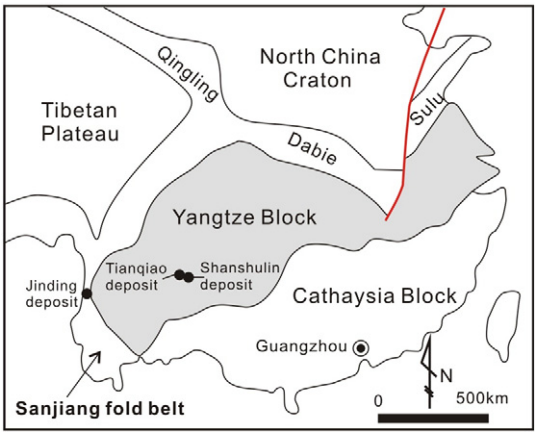

Fig. 9. The locations of Jinding, Shanshulin and Tianqiao Pb–Zn deposits in the southwestern China (modified from Xue et al., 2007). The Jinding deposit is located in the Sanjiang fold belt, whereas the Shanshulin and Tianqiao deposits are located in the western part of the Yangtze Block.

located in the Sanjiang fold belt (Fig. 9). The Jinding deposit is the largest Pb–Zn deposit in China, which has a metal reserve of 12.84 Mt (million tons) Zn with ore grade of 8.32–12.52% and 2.64 Mt Pb with ore grade of 1.16–2.42% (Xue et al., 2007). Orebodies commonly occur as stratified, lenticular, and irregular lenses in the sandstones, breccia-bearing sandstones, siltstones, and limestones of the Lower Cretaceous and Paleocene strata (Tang, 2013). Ores are mainly composed of pyrite, sphalerite, galena, anhydrite, calcite, quartz, and celestite (Fig. 10a).

The Shanshulin and Tianqiao Pb–Zn deposits in the western part of the Yangtze Block (Fig. 9) are hosted in Devonian and Carboniferous carbonate rocks (Gu, 2004; Zhou et al., 2013, 2014). The Shanshulin deposit has metal reserves of 0.27 Mt Pb + Zn with ore grades of 0.24–7.94% Pb and 1.09–26.64% Zn (Zhou et al., 2014), whereas the Tianqiao deposit contains 0.38 Mt Pb and Zn metals grading >15% Pb + Zn (Zhou et al., 2013). The two deposits have a similar mineral assemblage of pyrite, sphalerite, galena, calcite and dolomite (Fig. 10b–d). Petrographically, the mineralization sequence of different sulfide minerals in the Pb–Zn ores from the Shanshulin and Tianqiao deposits is pyrite, sphalerite and galena from early to late (Fig. 10b–d).

Germanium isotopic compositions of sphalerite, pyrite, and galena from the Jinding, Shanshulin and Tianqiao Pb–Zn deposits in southwestern China were obtained using the proposed method. The Ge concentrations and isotopic compositions of these sulfides, as well as other reported sulfides (Belissont et al., 2014; Escoube et al., 2012b; Luais, 2007, 2012) are compiled in Table 7 and are illustrated in Fig. 11.

The δ^{74}Ge values of sphalerite from the Jinding, Shanshulin, and Tianqiao Pb–Zn deposits in southwestern China range from −3.91‰ to 2.07‰ (Table 7). Pyrite from the three deposits shows a large variation of Ge isotopic compositions with δ^{74}Ge values ranging from −4.94‰ to 0.02‰ (Table 7 and Fig. 11). Germanium isotopic composition of galena from the Jinding and Shanshulin deposits shows the less variation of −0.75‰ to 0.21‰ (n = 3). In general, for the same ore with a paragenetic sequence of pyrite, sphalerite and galena from early to late, the δ^{74}Ge values of these sulfides follow the sequence of $\delta^{74}Ge_{pyrite} < \delta^{74}Ge_{sphalerite} < \delta^{74}Ge_{galena}$. This trend is probably attributed to a kinetic or Rayleigh fractionation that favors lighter Ge isotope incorporation in the earlier sulfides during subsequent fluid evolution and sulfide precipitation.

The Ge isotopic compositions of sphalerite from the MVT type Shanshulin and Tianqiao deposits (Gu, 2004) are basically similar to those of the Saint Salvy ZnS deposit, France (continental hydrothermal or metamorphosed ZnS deposit) (Marcoux et al., 1993; Munoz et al., 1994). Sphalerites from the Navan Pb–Zn deposit in Ireland (a volcanogenic sulfide deposit or MVT deposit) (Belissont et al., 2014; Blakeman et al., 2002; Everett et al., 2001; Symons et al., 2002), sandstone hosted Jinding Pb–Zn deposit (Xue et al., 2007), and modern seafloor hydrothermal systems (Escoube et al., 2012b; Rouxel et al., 2004) show similar low δ^{74}Ge values (about −4‰). Variable Ge isotopic compositions of sphalerites from different types of Pb–Zn deposits may be attributed to different mineralization temperatures, sources, and initial Ge content of hydrothermal fluids. The relative abundance of various minerals and the mineralization sequence may also lead to Ge isotope fractionation.

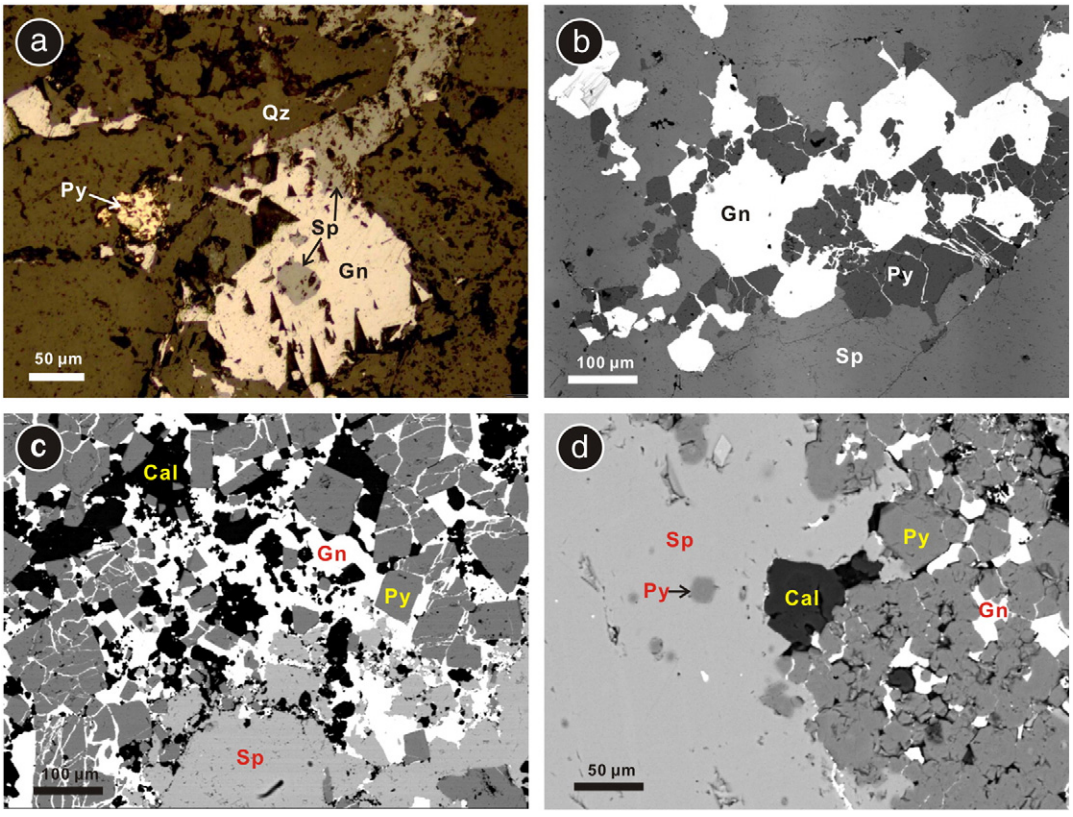

Fig. 10. (a) Ore from the Jinding Pb–Zn deposit composed of pyrite, sphalerite, galena, and quartz (under reflected light). Sphalerite was replaced by galena, indicating early formation of sphalerite; (b) ore from the Tianqiao Pb–Zn deposit comprising pyrite, sphalerite, and galena. Galena grows along the fracture of pyrite, indicating late formation of galena (BSE image); (c) ore from the Tianqiao Pb–Zn deposit consisting of pyrite, sphalerite, galena and calcite (BSE image). Pyrite was crosscut by galena and was replaced by sphalerite; indicating earliest formation of pyrite; (d) pyrite infilled and crosscut by galena for the ore from the Shanshulin Pb–Zn deposit (BSE image), also indicating the first formation of pyrite. Pyrite was enclosed in the sphalerite, also indicating the early formation of pyrite. Py, pyrite; Sp, sphalerite; Gn, galena; Cal, calcite; Qz, quartz.

Table 7
Germanium content and isotopic compositions of natural sulfide samples against NIST SRM 30120a.

Sample no.	Mineral	Ge (ppm)	δ^{74}Ge (‰)	2s	δ^{73}Ge (‰)	2s	δ^{72}Ge (‰)	2s	$\delta^{74/72}$Ge (‰)	2s	References
Jinding Pb–Zn deposit											
JDBC-2	Py	0.29	−0.10	0.20	0.17	0.18	0.03	0.16	−0.12	0.04	This study
Duplicate	Py		−0.02	0.08	0.26	0.25	−0.06	0.05	0.08	0.13	This study
JD-09-21	Sp	7.94	−3.83	0.04	−3.07	0.47	−1.93	0.05	−1.90	0.01	This study
JDJ-10-40	Py	0.34	−4.94	0.01	−3.15	0.08	−2.33	0.06	−2.61	0.05	This study
Duplicate	Py		−4.79	0.20	−2.91	0.12	−2.35	0.20	−2.45	0.01	This study
JD-09-44	Gn	0.34	−0.75	0.32	−0.23	0.13	−0.40	0.28	−0.35	0.04	This study
JD-09-55b	Sp	18.8	−3.91	0.04	−2.98	0.02	−2.02	0.06	−1.89	0.10	This study
Duplicate	Sp		−3.77	0.39	−2.87	0.17	−1.86	0.21	−1.92	0.18	This study
JD-09-63	Sp	10.9	−1.04	0.08	−0.87	0.04	−0.64	0.02	−0.40	0.10	This study
JD-09-58	Py	0.47	−2.38	0.15	−1.54	0.05	−1.14	0.23	−1.24	0.08	This study
Shanshulin Pb–Zn deposit											
SSL-1	Gn	1.70	0.21	0.09	0.25	0.14	0.16	0.07	0.05	0.02	This study
SSL-1	Sp	0.59	−1.41	0.18	−1.00	0.05	−0.73	0.14	−0.68	0.05	This study
SSL-2	Sp	0.21	0.32	0.28	0.21	0.09	0.19	0.22	0.13	0.06	This study
SSL-3	Gn	1.73	0.09	0.09	0.11	0.14	0.12	0.07	−0.03	0.02	This study
SSL-3	Sp	188	−1.13	0.28	−0.85	0.09	−0.57	0.22	−0.56	0.06	This study
SSL-4	Sp	197	−1.71	0.20	−1.34	0.24	−0.88	0.18	−0.83	0.02	This study
SSL-6	Py	2.70	−0.04	0.29	0.04	0.34	0.00	0.18	−0.04	0.11	This study
SSL-6	Sp	213	−1.13	0.12	−0.90	0.08	−0.56	0.07	−0.57	0.05	This study
SSL-6	Gn	2.40	−0.09	0.00	0.04	0.05	0.03	0.07	−0.11	0.07	This study
SSL-8	Sp	265	2.07	0.06	1.71	0.09	1.10	0.01	0.97	0.07	This study
Tianqiao Pb–Zn deposit											
TQ-8	Py	4.00	−0.01	0.16	0.70	0.11	−0.20	0.06	0.19	0.10	This study
TQ-8	Sp	36.2	0.54	0.17	0.54	0.42	0.29	0.10	0.24	0.07	This study
TQ-9	Sp	102	−1.63	0.03	−0.88	0.03	−0.92	0.02	−0.71	0.01	This study
TQ-10	Sp	77.5	−1.42	0.21	−0.83	0.03	−0.78	0.13	−0.64	0.08	This study
TQ-11	Sp	144	−0.99	0.15	−0.76	0.07	−0.51	0.05	−0.48	0.10	This study
TQ-12	Sp	152	0.02	0.14	−0.03	0.10	0.03	0.05	−0.01	0.09	This study
TQ-12-1	Py	0.21	−3.18	0.20	−1.80	0.30	−1.29	0.05	−1.89	0.15	This study
Navan Pb–Zn deposit											
U12473	Sp	77.5	−3.86	0.25							Escoube et al. (2012b)
U12474	Sp	144	−3.95	0.22							Escoube et al. (2012b)
U12487	Sp	152	−3.36	0.27							Escoube et al. (2012b)
U12487	Sp	6.00	−2.82	0.28							Escoube et al. (2012b)
U12499	Sp	28.0	−4.28	0.14							Escoube et al. (2012b)
Seafloor sulfide deposit											
FL-24-02	Sp	40.0	−3.26	0.15							Escoube et al. (2012b)
FL-19-08	Sp	45.0	−3.24	0.16							Escoube et al. (2012b)
ALV-2604-5-1A	Sp	159	−2.98	0.20							Escoube et al. (2012b)
FL-18-03/fond	Sp	200	−4.00	0.11							Escoube et al. (2012b)
Saint Salvy ZnS deposit											
62W	Sp	453	−0.74	0.15							Luais (2012)
64W	Sp	1047	−2.06	0.15							Luais (2012)
62E	Sp	813	−1.41	0.39	−1.17	0.20	−0.75	0.15			Belissont et al. (2014)
62W	Sp	908	−0.54	0.15	−0.59	0.17	−0.31	0.08			Belissont et al. (2014)
64W-02	Sp	699	−2.07	0.37	−1.63	0.28	−1.07	0.24			Belissont et al. (2014)
64W-08	Sp	240	−2.03	0.39	−1.63	0.34	−1.06	0.21			Belissont et al. (2014)
72W	Sp	470	−1.39	0.49	−1.18	0.47	−0.73	0.29			Belissont et al. (2014)
SAL-UN	Sp	925	0.64	0.23	0.40	0.21	0.32	0.06			Belissont et al. (2014)
K	Sp	1020	0.91	0.16	0.51	0.25	0.42	0.06			Belissont et al. (2014)

Note: Sp, sphalerite (ZnS); Py, pyrite (FeS_2); Gn, galena (PbS); 2s denote two times standard deviation.

5. Conclusions

A one step anion-exchange separation and purification process combined with HG-MC-ICP-MS can accurately measure Ge isotopic compositions of sphalerite, galena, pyrite, and chalcopyrite. The proposed method simplified the purification procedure and lowered the cost. The recoveries of Ge in sulfides of CRMC during the whole procedure were quantitatively assessed by the standard-addition method. The Ge isotope variations of natural sulfides (sphalerite, galena, and pyrite) from the Shanshulin, Tianqiao, and Jinding Pb–Zn deposits in SW China are up to about 7‰ in δ^{74}Ge. Sulfides have a mineral sequence of pyrite, sphalerite, and galena from early to late, which follows the trend of $\delta^{74}Ge_{pyrite} < \delta^{74}Ge_{sphalerite} < \delta^{74}Ge_{galena}$ for the same ore specimen, possibly induced by the process of kinetic or Rayleigh fractionation.

Acknowledgments

The authors acknowledge Zhang Jun of the First Institute of Oceanography, State Ocean Administration, China and Li Liang of the State Key Laboratory of Ore Deposit Geochemistry, Institute of Geochemistry, Chinese Academy of Sciences for their help during the analysis of Ge concentrations and Ge isotopic compositions. We thank Dr. Tang Yong-Yong for providing the sulfide samples of the Jinding deposit. We are grateful to Prof. F. M. Pirajno, Prof. Mei-Fu Zhou and two anonymous reviewers for their constructive comments which have significantly improved the manuscript. This project was financially supported by National Natural Science Foundation of China (grant no. 41073041) and Strategical Survey Program of the Tri-Rare Metal Resources of China (grant no. 12120113078200).

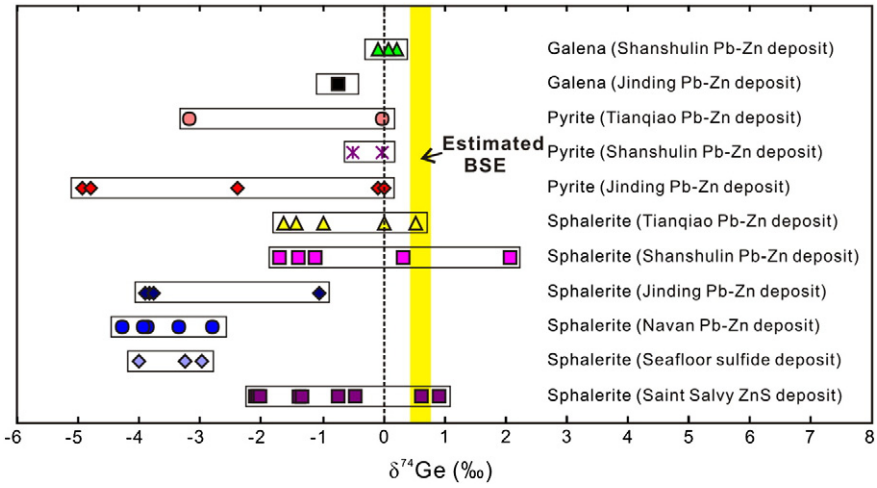

Fig. 11. Ge isotopic composition (δ^{74}Ge) of different sulfides from the Jinding, Shanshulin, and Tianqiao Pb–Zn deposits of SW China. The vertical bar represents the estimated Ge isotopic compositions of Bulk Silicate Earth (BSE) ($\delta^{74}Ge = 0.59 \pm 0.18$‰, Escoube et al., 2012b; $\delta^{74}Ge = 0.53 \pm 0.16$‰, Luais, 2012). The Ge isotopic compositions of sulfides from Navan, Saint Salvy and seafloor deposits were from Belissont et al. (2014), Escoube et al. (2012b), and Luais (2012).

Appendix A. The elemental concentration of four Chinese sulfide reference materials

Element	GBW-07267 Pyrite		GBW-07268 Chalcopyrite		GBW-07269 Galena		GBW-07270 Sphalerite	
	Certified Value	n	Certified Value	n	Certified Value	n	Certified Value	n
Ag	0.59 ± 0.13	8	846 ± 40	9	0.97* ± 0.02*	9	5.0 ± 0.4	9
As	(14.4)		(3.1)		5.3 ± 1.6	7	(3.3)	
Bi	2.9 ± 0.5	10	16.1 ± 2.4	10	1.4 ± 0.4	10	6.1 ± 1.2	9
Cd	0.71 ± 0.08	6	20.2 ± 1.0	8	16.5 ± 2.8	9	0.15* ± 0.01*	11
Co	(3.9)		75.1 ± 4.2	10	(0.4)		491 ± 23	12
Cu	431 ± 30	7	33.30* ± 0.17*	10	62.4 ± 2.5	8	0.10* ± 0.01*	11
Fe	46.08* ± 0.29*	10	30.30* ± 0.28*	10	127 ± 23	8	2.14* ± 0.14*	12
Ga	0.44 ± 0.14	6	(0.3)		(0.3)		251 ± 18	7
Ge	(0.2)				1.47 ± 0.26	6	6.0 ± 0.7	7
In			66.6 ± 4.8	7	0.29 ± 0.06	6	21.0 ± 1.4	6
Mn	28.9 ± 2.1	6	47.5 ± 3.7	8			169 ± 8.0	11
Ni	34.0 ± 2.7	8	41.3 ± 4.3	8			43.2 ± 4.0	8
Pb	(23.4)		128 ± 33	8	84.26* ± 0.36*	10	0.099* ± 0.013*	9
S*	52.7 2 ± 0.21	6	34.69 ± 0.19	7	13.3 ± 0.08	7	32.33 ± 0.17	7
Sb	1.1 ± 0.3	6	(2.7)		0.43* ± 0.07*	10	249 ± 56	8
Se	5.8 ± 0.7	9	48.3 ± 2.0	10			(3)	
Sn	(2.7)		(5.8)		0.11* ± 0.01*	6	(3.2)	
Te	0.95 ± 0.21	7	10.4 ± 2.7	9	(0.07)		(0.3)	
Tl					0.65 ± 0.10	6		
Zn	219 ± 17	9	0.30* ± 0.03*	10	533 ± 31	7	62.51* ± 0.17*	7

Note: n stands for number of sample; * means contents in percentage and unmarked numbers mean contents in ppm; () represents reference value; all errors are 1 s. Certified values are from RGSMRM (1995).

References

Belissont, R., Boiron, M.-C., Luais, B., Cathelineau, M., 2014. LA-ICP-MS analyses of minor and trace elements and bulk Ge isotopes in zoned Ge-rich sphalerites from the Noailhac-Saint-Salvy deposit (France): insights on incorporation mechanisms and ore deposition processes. Geochim. Cosmochim. Acta 126, 518–540.

Bernstein, L.R., 1985. Germanium geochemistry and mineralogy. Geochim. Cosmochim. Acta 49, 2409–2422.

Blakeman, R.J., Ashton, J.H., Boyce, A.J., Fallick, A.E., Russell, M.J., 2002. Timing of interplay between hydrothermal and surface fluids in the Navan Zn + Pb orebody, Ireland: evidence from metal distribution trends, mineral textures, and δ^{34}S analyses. Econ. Geol. 97, 73–91.

Chetty, D., Frimmel, H., 2000. The role of evaporites in the genesis of base metal sulphide mineralisation in the Northern Platform of the Pan-African Damara Belt Namibia: geochemical and fluid inclusion evidence from carbonate wall rock alteration. Mineral. Deposita 35, 364–376.

Dedina, J., Tsalev, D.L., Winefordner, J., 1995. Hydride Generation Atomic Absorption Spectrometry. Wiley, New York p. 526.

Escoube, R., Rouxel, O., Donard, O., 2008. Measurement of Germanium isotope composition in marine samples by hydride generation coupled to MC-ICP-MS EGU General Assembly. Geophys. Res. Abstr. 12035.

Escoube, R., Rouxel, O.J., Donard, O.F.X., 2012a. Coupled Ge/Si and Ge isotope ratios as new geochemical tracers of seafloor hydrothermal systems: a case study at Loihi Seamount. Geochim. Cosmochim. Acta Suppl. 76, 1305.

Escoube, R., Rouxel, O.J., Luais, B., Ponzevera, E., Donard, O.F., 2012b. An intercomparison study of the germanium isotope composition of geological reference materials. Geostand. Geoanal. Res. 36, 149–159.

Everett, C.E., WIkinsonI, J.J., Boyce, A.J., Gleeson, S.A., 2001. The role of bittern brines and fluid mixing in the genesis of the Navan Zn–Pb deposit, Ireland. GSA Annual Meeting (November 5–8).

Frenzel, M., Ketris, M.P., Gutzmer, J., 2014. On the geological availability of germanium. Mineral. Deposita 49, 471–486.

Galy, A., Pomiès, C., Day, J.A., Pokrovsky, O.S., Schott, J., 2003. High precision measurement of germanium isotope ratio variations by multiple collector-inductively coupled plasma mass spectrometry. J. Anal. At. Spectrom. 18, 115–119.
Green, M., Rosman, K., De Laeter, J., 1986. The isotopic composition of germanium in terrestrial samples. Int. J. Mass Spectrom. Ion Processes 68, 15–24.
Gu, S.Y., 2004. Characteristics of rare-earth elements composition within lead–zinc deposits in northwestern Guizhou: in addition to a discussion of relationship between lead–zinc deposits and Emeishan basalts in northwestern Guizhou. Guizhou Geol. 23, 274–277 (in Chinese with English Abstract).
Hirata, T., 1997. Isotopic variations of germanium in iron and stony iron meteorites. Geochim. Cosmochim. Acta 61, 4439–4448.
Kampunzu, A., Cailteux, J., Kamona, A., Intiomale, M., Melcher, F., 2009. Sediment-hosted Zn–Pb–Cu deposits in the Central African Copperbelt. Ore Geol. Rev. 35, 263–297.
Kipphardt, H., Valkiers, S., Henriksen, F., De Bievre, P., Taylor, P.D.P., Tolg, G., 1999. Measurement of the isotopic composition of germanium using GeF_4 produced by direct fluorination and wet chemical procedures. Int. J. Mass Spectrom. 189, 27–37.
Li, C.Y., Liu, Y.P., Zhang, Q., Pi, D.H., Zhang, W.L., Chen, J., 2005. Discovery of antimony and distribution characteristics of associated elements in Huize Pb–Zn deposit. Miner. Depos. 24, 52–60 (in Chinese with English abstract).
Li, X.-F., Zhao, H., Tang, M., Liu, Y., 2009. Theoretical prediction for several important equilibrium Ge isotope fractionation factors and geological implications. Earth Planet. Sci. Lett. 287, 1–11.
Liu, Y.J., Cao, L.M., Li, Z.L., 1984. Elements Geochemistry. Science Press, Beijing pp. 332–333 (in Chinese).
Lobo, L., Degryse, P., Shortland, A., Vanhaecke, F., 2013. Isotopic analysis of antimony using multi-collector ICP-mass spectrometry for provenance determination of Roman glass. J. Anal. At. Spectrom. 28, 1213–1219.
Luais, B., 2007. Isotopic fractionation of germanium in iron meteorites: significance for nebular condensation, core formation and impact processes. Earth Planet. Sci. Lett. 262, 21–36.
Luais, B., 2012. Germanium chemistry and MC-ICPMS isotopic measurements of Fe–Ni, Zn alloys and silicate matrices: insights into deep Earth processes. Chem. Geol. 334, 295–311.
Luais, B., Framboisier, X., Carignan, J., Ludden, J., 2000. Analytical development of Ge isotopic analyses using multi-collection plasma source mass spectrometry: isoprobe MC-HEX-ICP-MS (micromass). Geoanalysis 45–46 (Pont-A Mousson (France)).
Marcoux, E., Cassard, D., CHABOD, J.C., 1993. Source hercynienne du gisement filonien Zn (Ge) de Saint-Salvy (Tarn, France). Comptes rendus de l'Académie des sciences. Série 2 Mécanique, Physique, Chimie, Sciences de l'univers, Sciences de la Terre 316, 1091–1098.
Melcher, F., Oberthur, T., Rammlmair, D., 2006. Geochemical and mineralogical distribution of germanium in the Khusib Springs Cu–Zn–Pb–Ag sulfide deposit, Otavi Mountain Land Namibia. Ore Geol. Rev. 28, 32–56.
Munoz, M., Boyce, A.J., Courjault-Rade, P., Fallick, A.E., Tollon, F., 1994. Multi-stage fluid incursion in the Palaeozoic basement-hosted Saint-Salvy ore deposit (NW Montagne Noire, Southern France). Appl. Geochem. 9, 609–626.
Nishimura, H., Takeshi, H., Okano, J., 1988. Isotopic abundances of germanium determined by secondary ion mass spectrometry. Mass Spectrom. 36, 197–202.
Qi, L., Hu, J., Gregoire, D.C., 2000. Determination of trace elements in granites by inductively coupled plasma mass spectrometry. Talanta 51, 507–513.
Qi, H.-W., Rouxel, O., Hu, R.-Z., Bi, X.-W., Wen, H.-J., 2011. Germanium isotopic systematics in Ge-rich coal from the Lincang Ge deposit, Yunnan, Southwestern China. Chem. Geol. 286, 252–265.
Reynolds, J.H., 1953. The isotopic constitution of silicon, germanium, and hafnium. Phys. Rev. 90, 1047–1049.
RGSMRM (Research Group of Sulfide Mineral Reference Materials), 1995. The preparation of sulphide mineral reference materials. Rock Miner. Anal. 14, 81–113 (in Chinese with English Abstract).
Richter, F.M., Liang, Y., Davis, A.M., 1999. Isotope fractionation by diffusion in molten oxides. Geochim. Cosmochim. Acta 63, 2853–2861.
Rosman, K.J.R., Taylor, P.D.P., 1998. Isotopic compositions of the elements 1997. J. Phys. Chem. Ref. Data 27, 1275–1288.
Rouxel, O., Fouquet, Y., Ludden, J.N., 2004. Subsurface processes at the lucky strike hydrothermal field, Mid-Atlantic ridge: evidence from sulfur, selenium, and iron isotopes. Geochim. Cosmochim. Acta 68, 2295–2311.
Rouxel, O., Galy, A., Elderfield, H., 2006. Germanium isotopic variations in igneous rocks and marine sediments. Geochim. Cosmochim. Acta 70, 3387–3400.
Rouxel, O.J., Escoube, R., Donard, O.F.X., 2008. Measurement of Germanium isotope composition in marine samples by hydride generation coupled to MC-ICP-MS. Geochim. Cosmochim. Acta Suppl. 72, 809.
Shima, M., 1963. Isotopic composition of germanium in meteorites. J. Geophys. Res. 68, 4289–4992.
Siebert, C., Ross, A., McManus, J., 2006. Germanium isotope measurements of high-temperature geothermal fluids using double-spike hydride generation MC-ICP-MS. Geochim. Cosmochim. Acta 70, 3986–3995.
Slack, J.F., Kelley, K.D., Anderson, V.M., Clark, J.L., Ayuso, R.A., 2004. Multistage hydrothermal silicification and Fe–Tl–As–Sb–Ge-REE enrichment in the Red Dog Zn–Pb–Ag district, northern Alaska: geochemistry, origin, and exploration applications. Econ. Geol. 99, 1481–1508.
Symons, D., Smethurst, M., Ashton, J., 2002. Paleomagnetism of the Navan Zn–Pb deposit Ireland. Econ. Geol. 97, 997–1012.
Tang, Y.Y., 2013. Abnormal Enrichment Mechanisms of Ore-forming Metals in the Jinding Zn–Pb Deposit, Yunnan Province, China. (PhD thesis) University of Chinese Academy of Sciences, Beijing (in Chinese with English abstract).
Tipper, E.T., Louvat, P., Capmas, F., Galy, A., Gaillardet, J., 2008. Accuracy of stable Mg and Ca isotope data obtained by MC-ICP-MS using the standard addition method. Chem. Geol. 257, 65–75.
Xue, C.J., Zeng, R., Liu, S.W., Chi, G.X., Qing, H.R., Chen, Y.C., Yang, J.M., Wang, D.H., 2007. Geologic, fluid inclusion and isotopic characteristics of the Jinding Zn–Pb deposit, western Yunnan South China: a review. Ore Geol. Rev. 31, 337–359.
Yang, L., Meija, J., 2010. Resolving the germanium atomic weight disparity using multicollector ICPMS. Anal. Chem. 82, 4188–4193.
Yang, L., Mester,, Z.n, Zhou, L., Gao, S., Sturgeon, R.E., Meija, J., 2011. Observations of large mass-independent fractionation occurring in MC-ICPMS: implications for determination of accurate isotope amount ratios. Anal. Chem. 83, 8999–9004.
Zhou, J., Huang, Z., Zhou, M., Li, X., Jin, Z., 2013. Constraints of C–O–S–Pb isotope compositions and Rb–Sr isotopic age on the origin of the Tianqiao carbonate-hosted Pb–Zn deposit SW China. Ore Geol. Rev. 53, 77–92.
Zhou, J.-X., Huang, Z.-L., Zhou, M.-F., Zhu, X.-K., Muchez, P., 2014. Zinc, sulfur and lead isotopic variations in carbonate-hosted Pb–Zn sulfide deposits, southwest China. Ore Geol. Rev. 58, 41–54.